

Review

Photocatalytic TiO₂-Based Nanostructured Materials for Microbial Inactivation

Ilaria De Pasquale ¹, Chiara Lo Porto ¹, Massimo Dell'Edera ^{1,2}, Francesca Petronella ³,
Angela Agostiano ^{1,2}, Maria Lucia Curri ^{1,2,*} and Roberto Comparelli ^{1,*}

¹ CNR-IPCF, Istituto per i Processi Chimico-Fisici, S.S. Bari, c/o Dip. Chimica Via Orabona 4, 70126 Bari, Italy; i.depasquale@ba.ipcf.cnr.it (I.D.P.); c.loporto@ba.ipcf.cnr.it (C.L.P.); m.delledera@ba.ipcf.cnr.it (M.D.); angela.agostiano@uniba.it (A.A.)

² Dipartimento di Chimica, Università degli Studi di Bari Aldo Moro, Via Orabona 4, 70126 Bari, Italy

³ CNR—IC, Istituto di Cristallografia, S.S. Roma, Via Salaria Km 29,300, 00015 Rome, Italy; f.petronella@ba.ipcf.cnr.it

* Correspondence: marialucia.curri@uniba.it (M.L.C.); roberto.comparelli@cnr.it (R.C.); Tel.: +39-080-5442027 (R.C.)

Received: 12 October 2020; Accepted: 23 November 2020; Published: 26 November 2020



Abstract: Pathogenic microorganisms can spread throughout the world population, as the current COVID-19 pandemic has dramatically demonstrated. In this scenario, a protection against pathogens and other microorganisms can come from the use of photoactive materials as antimicrobial agents able to hinder, or at least limit, their spreading by means of photocatalytically assisted processes activated by light—possibly sunlight—promoting the formation of reactive oxygen species (ROS) that can kill microorganisms in different matrices such as water or different surfaces without affecting human health. In this review, we focus the attention on TiO₂ nanoparticle-based antimicrobial materials, intending to provide an overview of the most promising synthetic techniques, toward possible large-scale production, critically review the capability of such materials to promote pathogen (i.e., bacteria, virus, and fungi) inactivation, and, finally, take a look at selected technological applications.

Keywords: TiO₂; photocatalysis; nanoparticles; pathogens; bacteria; virus; fungi

1. Introduction

Over the last decades, titanium dioxide (TiO₂) has been extensively investigated for its physical-chemical properties, that, combined with its high stability, low cost, and safety for the environment and humans, have resulted in a range of environmental and energy applications.

When TiO₂ is obtained at nanoscale, many relevant properties of this semiconductor are enhanced, due to the increased surface area, which results from the high surface-to-volume ratio, the excellent surface morphology, and the band edge modulation, that, overall, turn into a control on the photocatalytic behavior and performance of the nanostructured materials [1–3].

Upon illumination, TiO₂ nanoparticles (NPs) convert incoming photons into excitons, or electron/hole pairs, which can migrate to the surface and participate in redox reactions and generate reactive oxygen species (ROS), such as hydroxyl radicals (OH·) and superoxide(O₂[−]) [3,4].

Indeed, the photocatalytic behavior of TiO₂ NPs has been widely exploited for removal of water and air contaminants and self-cleaning surfaces [1–4]. Currently, increasing concerns regarding the COVID-19 pandemic are drawing the attention of researchers and general public more and more to photocatalytic antimicrobial and antiviral treatments with the purpose of hindering virus spreading, by using light (possibly solar light) activated systems.

TiO₂ NPs are among the most studied materials in the area of photocatalytic antimicrobial applications, having demonstrated a great potential for the disinfection/inactivation of harmful

pathogens, including bacteria, viruses, and fungi [5]. However, aside from the superior advantage of TiO₂ nanostructured materials, some drawbacks have been identified, i.e., high recombination rate of the photogenerated species and limited solar light sensitivity, therefore various modifications have been developed to enhance the photocatalytic efficiency [3,4].

Upon photoactivation of TiO₂ NPs, the biocidal action is a result of the modulation of charge carriers, electrons, and holes at the surface of the material, resulting in powerful and long-lasting capabilities [1], since the process does not rely on the release of metal ions, and hence the material consumption, as it happens in the case of Ag-based antimicrobial material. Moreover, TiO₂ NPs-based systems have a substantial advantage due to their non-contact biocidal action. Finally, since any possible release into the environment of potentially toxic NPs—with unpredictable effects on human health—from the material or device for the final application must be prevented, the TiO₂-based structures are required to be suited for immobilization onto substrate and/or incorporation in matrices. In this regard, this class of materials could be considered reasonably environmentally friendly.

The antimicrobial activity of TiO₂ NPs is primarily attributed to the photocatalytic generation, under band-gap irradiation, of ROS with high oxidative potentials. However, other possible factors may be considered to explain their biocidal effect, such as free metal ions formation or synergistic effects deriving from the combination of TiO₂ NPs with other materials and compounds in nanocomposite systems [1,2,5].

In the following, possible mechanisms underlying the antimicrobial behavior of the TiO₂ NPs-based systems will be described, specifically highlighting the photocatalytic path, along with other possible alternative factors, that, also synergistically combined, can be responsible for microorganism inactivation.

The biocidal activity of TiO₂ NPs-based materials is greatly dependent on their photocatalytic performance, which is strongly influenced by several inherent factors, including the NP morphology, size, chemistry, crystalline phase, structure, and precursor, as well as their possible modification with metals, other semiconductors, and organic compounds [5].

For this reason, here the latest tendencies on synthesis of TiO₂ NPs-based materials will be illustrated, specifically addressing environmentally sustainable and ecological processes (i.e., requiring mild reaction conditions and non-toxic precursors) and scalable preparation procedures, such as sol-gel and hydrothermal methods. Nanocomposites preparation, including TiO₂/metal nanocomposites, and in particular, TiO₂-/Ag-based ones, and nanocomposites coupling TiO₂ with other metals and metal oxides, but also with organic and even biological molecules, will be reviewed in order to explore the effect of the nanostructured material features on the overall performance. Then, the activity of TiO₂ nanosized-based systems against bacteria, fungi, and viruses, in that order, will be presented, highlighting the effect of different biological factors on their overall antimicrobial performances, including cell membrane structure, metabolism, physiological state of the cells, and environmental stress. Finally, selected applications of the antimicrobial TiO₂-based nanomaterials will be described, namely, environmental applications, including water treatment, anti-biofouling membranes for water treatment and disinfection of building materials, and disinfection of biomaterial and of materials for food packaging and processing. The ability to push forward the great potential of the TiO₂ nanostructured materials as an antimicrobial system is strongly motivated by the need for inorganic alternatives to antibiotics, due also to the emergent multidrug resistance of some bacteria and the toxicity to the human body of some organic antimicrobial substances. Advances in preparative approaches, alongside a further elucidation and a more comprehensive understanding of the mechanisms underlying the functions of TiO₂-based nanostructures, could provide additional and powerful tools to tackle the enormous incidence of bacteria and viruses and strengthen also the capacity to inactivate and destroy a wide range of microorganisms, possibly extending their biocidal action to extremely harmful strains like the SARS-CoV viruses.

2. Preparation of TiO₂-Based Nanostructured Materials for Photocatalytic Inactivation of Microorganisms

2.1. Synthesis of Photocatalytic TiO₂ Nanoparticles with Antimicrobial Function

For decades, nanosized TiO₂ has been widely investigated because of its unique photocatalytic properties. Among the wide range of environmental applications enabled by such a material at nanoscale, the photocatalytic inactivation of harmful microorganisms is attracting increasing attention.

In the last years, many studies have described the antimicrobial activity of commercially available TiO₂ NPs. However, more recently, innovative approaches aiming at the synthesis of original TiO₂-based nanomaterials, specifically designed for photocatalytically assisted inactivation of bacteria and viruses, have been reported.

Such approaches vary in terms of degree of complexity and production cost, and allow access to photocatalytic TiO₂-based nanomaterials with purposely selected physical-chemical properties, including controlled dimension and geometry, and thus size-dependent characteristics, engineered surface chemistry, enhanced colloidal stability even in different conditions of ionic strength, and biocompatibility, especially for application in the field of health care and food preservation.

In the literature, a plethora of synthetic routes has been proposed for the preparation of nanosized TiO₂ with photocatalytic antimicrobial properties; here we focus our attention on sol-gel and hydrothermal methods (Figure 1), as they have been regarded, so far, among the promising techniques for the large scale production of TiO₂ NPs, owing to their user- and environment- friendly and cost effective procedures [6–9]. However, for the sake of brevity, herein we report only a small selection of the numerous examples reported in literature and we direct the readers to more specific papers [8,10,11].

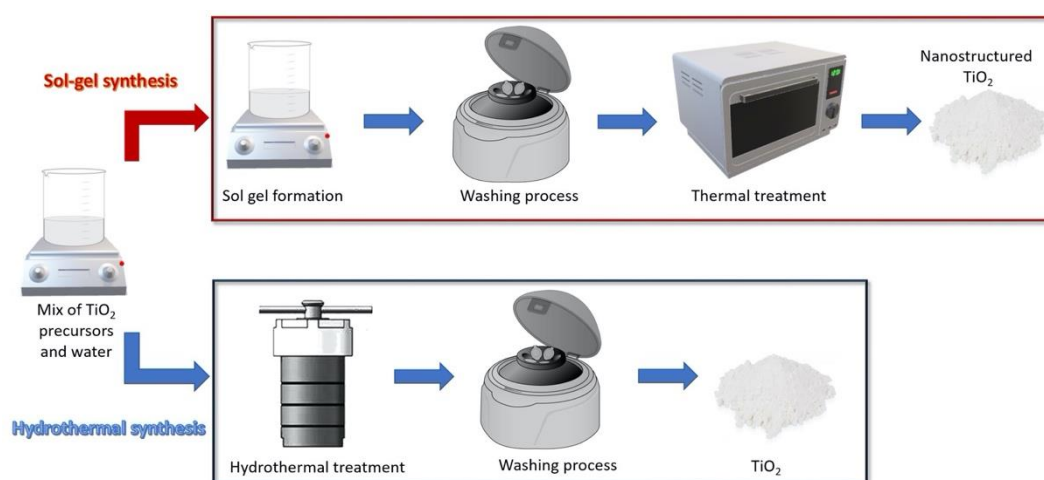


Figure 1. Schematic representation of TiO₂ NPs sol-gel method (upper panel) and hydrothermal synthetic approach (lower panel).

2.1.1. Sol-Gel Methods

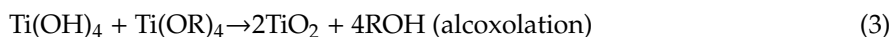
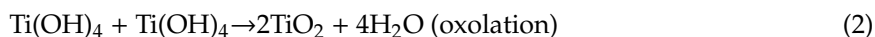
The sol-gel method is based on the conversion of “sol(s)”, namely solid particles suspended in a liquid, into a network of sols defined as “gel”, containing both a liquid phase and a solid phase. Figure 1 shows a schematic representation of a general procedure typically followed for a common sol-gel synthesis. In the first step, the TiO₂ precursor is dissolved in water, in an alcohol (e.g., methanol, ethanol, or isopropanol) or in a defined mixture of alcohol and water as a reaction solvent. Commonly used TiO₂ precursors include (but are not limited to) titanium (IV) butoxide (Ti(OBu)₄), titanium (III) chloride (TiCl₃), titanium (IV) tetrachloride (TiCl₄), and titanium (IV) isopropoxide (Ti[OCH(CH₃)₂]₄, TTIP). At this stage, the formation of TiO₂ takes place through the two main reactions of hydrolysis (Equation (1)) and condensation (Equations (2) and (3)). Subsequently, in most reported protocols,

the obtained product is thermally treated in order to obtain TiO₂ NPs with a defined size and crystalline phase [12–15].

Hydrolysis:



Condensation:



In the reactions (1) and (3), R represents organic functional group of the organometallic TiO₂ precursor, such as ethyl, i-propyl, n-butyl. The dilution of the TiO₂ precursor in the alcohol and/or in water before being added to the selected reaction solvent is useful to control the reaction rate of the hydrolysis process by slowing down the reaction rate as the dilution of the precursors increase. In the sol-gel method, the synthesis parameters affecting the properties and structure (crystalline phase(s)) of the resulting TiO₂ NPs photocatalyst are: H₂O/TiO₂ precursor ratio, pH value measured during the synthesis, and experimental conditions of possible calcination step.

Vargas et al., starting from the Ti(OBu)₄ as a precursor, performed a sol gel synthesis consisting of two steps: firstly, the Ti(OBu)₄ was dispersed in ethanol and allowed to stir in distilled water. Then, the obtained product was dried before being thermally treated for 2 h, at increasing temperature, 350 °C, 400 °C, and 770 °C. As a result, X-ray diffraction (XRD) analysis demonstrated that a different crystalline composition was attained as a function of the thermal treatment temperature. In particular, the obtained material was found amorphous after the treatment at 350 °C, while anatase was the main crystalline phase at 400 °C, and finally the treatment at 770 °C resulted in rutile as the single crystalline phase. Scanning (SEM) and transmission (TEM) electron microscopy analysis highlighted a morphology (Figure 2) characterized by the presence of primary sub-micrometric spheroidal particles with different average sizes, namely 100 nm for the amorphous product, and 50 nm for the two crystalline samples. The thermal treatment conditions were found to also affect the specific surface area value [16] of the resulting nanomaterials, as the increase in temperature resulted in a decrease of the specific surface area [17].

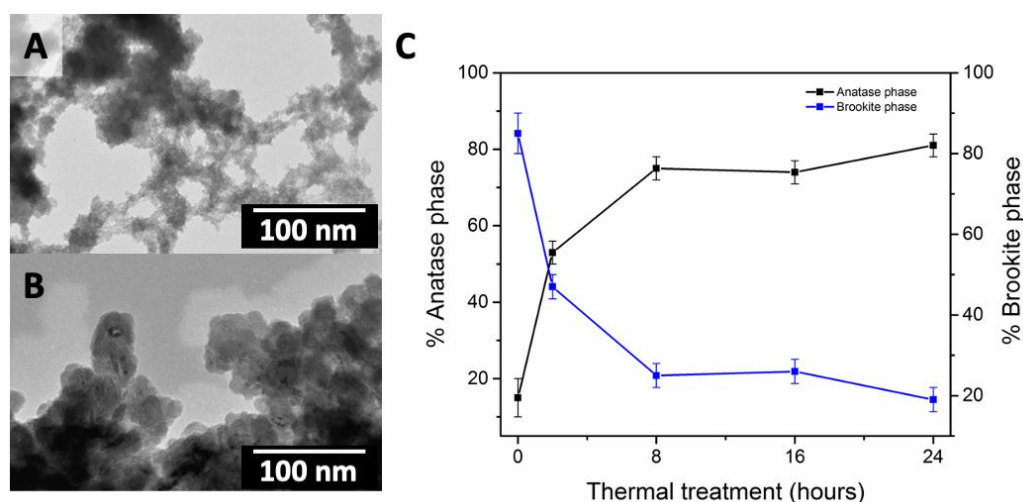


Figure 2. Transmission electron microscopy (TEM) micrographs of synthesized TiO₂ nanoparticles (NPs) before (A) and after the thermal treatment at 110 °C in an oven carried out for 16 h (B). Panel (C) percentage of anatase and brookite phase in different samples estimated by quantitative phase analysis by X-ray diffraction (XRD) pattern as a function of thermal treatment duration time at 110 °C. Reprinted with permission from ref. [16].

Dell'Edera et al. pointed out the correlation between TiO₂ heat treatment and the morphological properties of the obtained nanomaterial. The synthesis was carried out by precipitation of TiOSO₄ in an aqueous solution of NH₄HCO₃. The obtained sol was thermally treated in an oven at 110 °C for 16 h. SEM micrographs (Figure 2 panel A-B) show that small NPs were present in the untreated sample (~1 nm); after the heat treatment larger NPs were visible (23 ± 6 nm). Furthermore, Figure 2 panel C shows that the crystalline phase changed and a trend of the crystalline phase composition was observed as a function of the extent of heat treatment conditions. Initially there was a predominance of the brookite phase, then, during the thermal treatment the brookite phase progressively converted into the anatase phase. The specific surface area (SSA) depended on the thermal treatment conditions; in particular, for untreated TiO₂ NPs an SSA of 503.0 m²/g was measured, while treated NPs resulted in an SSA of 336.5 m²/g. The obtained TiO₂ NPs were found to be photocatalytically active, thus a potential candidate for antimicrobial applications. The dependence of the photocatalytic performance on properties such as crystalline phase composition, surface chemistry, and surface area was also highlighted [16].

In the sol-gel routes, the hydrolysis reaction, necessary for the formation of TiO₂, is acid catalyzed [18,19]. It follows that pH is a critical parameter in the synthesis that has been also found to influence morphological and structural properties of the resulting nanomaterial. Indeed, Ibrahim et al. demonstrated that alkaline conditions (pH 9) promote anatase structure, while higher acidity (pH < 5) results in rutile phase [20].

On the other hand, Galkina et al. synthesized anatase and brookite nanocrystalline TiO₂ using a sol-gel process by working at acid pH [21]. TTIP was dissolved in isopropyl alcohol and then added to an aqueous medium acidified by nitric acid. The obtained sol was used to modify cotton fibers, thus obtaining an antibacterial composite material. Cotton fibers were pre-treated in order to anchor the TiO₂ NPs therein. In particular, a spacer, a cyclic anhydride, prepared by the reaction between 1,2,3,4-butanetetracarboxylic acid (BTCA) and NaH₂PO₂ in a water solution, was inserted at the fiber surface. Once pre-treated, the cotton fibers were functionalized with TiO₂ NPs by adding them to the aqueous solution and heating at 70 °C for 2 h. The presence of nitric acid in the preparation of the sol was found able to drive the NP growth toward the formation of both brookite and anatase, single phase, TiO₂ NPs. The obtained cotton/TiO₂ composites demonstrated high bacteriostatic effects against *Escherichia coli* (*E. coli*) [21].

The solvent used to disperse the TiO₂ precursor may also affect the physical-chemical characteristics of TiO₂ NPs prepared by using a sol-gel method. Indeed, the morphology of the TiO₂ NPs was found to be influenced by the volume ratio between alcohol and TiO₂ precursor, as well as by the nature of alcohol selected as a solvent for the specific synthetic route. As an example, Bahar et al. reported that syntheses performed in ethanol lead to larger NPs (33 nm) than those obtained in butanol (26 nm) and isopropanol (30 nm) [22]. Duymaz et al. investigated the effect of the solvent composition, testing two different solvents (ethyl alcohol or water) to dissolve the TiO₂ precursor. After preparing the precursor in water and alcohol solution, respectively, its oxidation was catalyzed by the addition of nitric acid to the two systems and, for both of them, the sol-gel reaction was carried out at 50 °C to obtain a homogeneous dispersion. Then, the TiO₂ gel was dried for 24 h at 90 °C and finally ground to obtain fine powders, which were analyzed using a dynamic light scattering (DLS) technique. The use of ethanol was found to induce the formation of aggregates of TiO₂ NPs smaller (1858 nm) than those obtained by using water (2641 nm). The report indicated that the smaller TiO₂ aggregates, thanks to their size, were found to be optimal for being supported on several substrates such as silica, calcite, talc, and zinc borate. The immobilization of TiO₂ on each of these substrates was performed directly in situ, by simply adding the supporting material in the reaction mixture where the oxidation reaction takes place. The obtained NPs showed antibacterial behavior against *E. coli* and *Staphylococcus aureus* (*St. aureus*) [23].

2.1.2. Hydrothermal Methods

Hydrothermal (HT) synthesis, along with sol-gel process, is also a very common method for preparing TiO₂-based nanomaterials. In hydrothermal synthesis, that is, a solution approach, the formation of nanomaterials can take place in a wide range of temperatures, from room temperature to high temperatures (up to 400 °C [8]). Pressure can also be relevant in HT reaction, as it enables the control of morphology for the resulting nanomaterial. In a HT reaction, either low-pressure or high-pressure conditions can be applied, depending on the vapor pressure of the most abundant component of the reaction mixture under the investigated experimental conditions. Therefore, generally, a HT synthesis is carried out in an autoclave reactor, where it is essential to carefully control pressure and temperature.

The scheme of a typical HT synthetic procedure is depicted in Figure 1. In the first step, a mixture of water and TiO₂ precursor is prepared; then the obtained solution is transferred in the autoclave reactor, setting specific temperature pressure conditions. At this stage, the hydrolysis and condensation reactions take place, forming a three-dimensional network, similar to what happens in a sol-gel process. HT processes can be regarded as a sort of evolution of the synthetic sol-gel processes, because they allow one to obtain NPs with a high degree of crystallinity in fewer and simpler steps relative to the procedures typically realized for the sol-gel methods.

Rasheed et al. proposed a procedure to obtain rutile phase TiO₂ NPs starting from a sol obtained by mixing TiCl₄, deionized water, and ethanol. The dispersion was kept under vigorous stirring for 30 min until it became colorless, then, it was introduced into a Teflon-lined stainless-steel autoclave. The autoclave was sealed and placed in an oven at 200 °C for 6 h. The XRD analysis confirmed the presence of rutile as a single crystalline phase in the resulting materials. The photocatalytic antibacterial behavior was investigated against *E. coli* and *St. aureus* [24].

Varying the synthetic parameter of the HT procedure was also possible to obtain nanomaterials with a more complex morphology, such as the flower like nanostructures, composed by rod-like TiO₂ NPs reported by Korosi et al. [25]. A sol dispersion was obtained by mixing distilled water and TiCl₄ previously dissolved in 2-propanol. The resulting colorless dispersion was aged for two weeks at room temperature without stirring and then left to react in autoclave, for 12 h at increasing temperature values, namely 150 °C, 200 °C, and 250 °C. The HT reaction temperature affected both the structure and the specific surface area of the obtained material. Indeed, as the temperature increased, a decrease of the specific surface area was observed, along with an increase of the rutile amount up to the 100% after treatment for 12 h at 250 °C [25]. Further, SEM micrographs (Figure 3) pointed out that the crystallite size increased with the HT treatment temperature. The obtained material was effective in the photocatalytic inactivation of *Klebsiella pneumoniae* (*K. pneumoniae*).

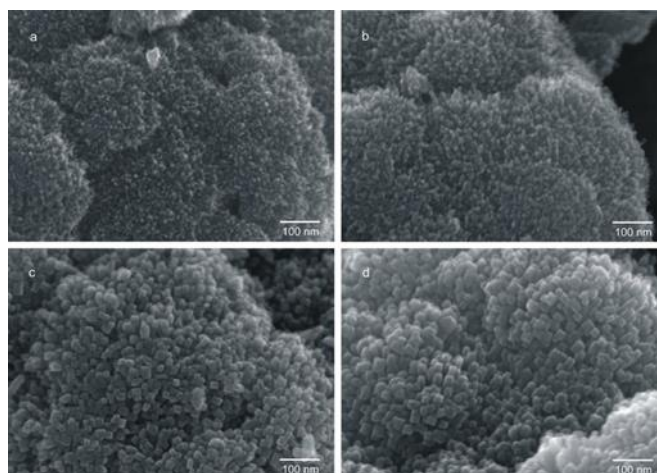


Figure 3. High-resolution scanning electron microscopy (SEM) micrographs of flower-like rutile TiO₂ (FLH-R-TiO₂): (a) FLH-R-TiO₂/AP (as prepared), (b) FLH-R-TiO₂/150, (c) FLH-R-TiO₂/200 and (d) FLH-R-TiO₂/250. Reprinted from ref. [25], Copyright (2016), with permission from Elsevier.

The HT process can also be conveniently tuned to modify the morphology of pre-synthesized TiO₂ NPs, as reported by Leon-Rios et al., who demonstrated the conversion of spherical TiO₂ NPs into TiO₂ nanowires obtained by means of a HT treatment. In detail, a water suspension of TiO₂ and NaOH was introduced in a Teflon-lined autoclave reactor and heated for 6 days at a temperature of 130 °C. The resulting powder was washed with HCl, then calcined at 500 °C leading to nanowires of TiO₂ in monoclinic phase, a metastable phase usually called TiO₂-B. TiO₂-B crystalline structure is characterized by a degree of exposure of TiO₂ (010) facets higher than that found in anatase, rutile, or brookite crystalline phase. Such TiO₂ (010) facets are known to be more photocatalytically active than other TiO₂ facets, thus making TiO₂-B a valuable candidate for photocatalytic applications [26,27]. As an example, TiO₂-B demonstrated effective in the UV induced inactivation of *E. coli* [27].

2.2. Preparation of TiO₂/Metal Nanocomposites

The increasing demand for highly efficient, visible-light-active photocatalysts can be addressed by designing and realizing hybrid nanostructured materials formed of two or more components, each characterized by peculiar size dependent properties, surface chemistry, and morphology, that are combined into one nano-object with unprecedented chemical–physical characteristics. Indeed, the presence of a metallic domain coupled to TiO₂ leads to a nanomaterial particularly suited for accomplishing visible light photocatalysis, as, extending the absorption ability of TiO₂ in the visible, the capacity to convert solar energy into chemical energy is increased. Several papers have demonstrated a significant enhancement in visible-light-driven photocatalytic efficiency of nanocomposites obtained upon deposition of Ag and Au NPs onto TiO₂ nanostructures [3,4,28]. These composite materials are also very interesting due to the ability of metal NPs to convey bactericidal properties to the system even in the dark, thanks to the slow release of a small amount of metal ions that are known to be toxic for pathogens even at ppm level.

2.2.1. TiO₂/Ag-Based Nanocomposites

One of the most investigated methods to improve the biocidal activity of TiO₂ against bacteria and viruses, enhancing at the same time its photocatalytic activity in the visible range, consists of modifying TiO₂ with Ag NPs thus obtaining TiO₂/Ag-based nanocomposites with unique photocatalytic and antibacterial properties [29]. Remarkably, in metal/semiconductor-based nanocomposites the interaction between semiconductors and metal NPs, under UV or visible light irradiation affects the properties of the resulting nanocomposite [3]. Indeed, the role played by the metal NPs in influencing

the energetics of the system, leading to an enhanced photoinduced charge separation, has been extensively investigated especially with respect to the photocatalytic reactions [30].

Several methods have been reported for the preparation of TiO₂/Ag-based nanocomposites with combined antibacterial and photocatalytic properties. Sol-gel processes, that allow one to simultaneously synthesize TiO₂ NPs and Ag NPs, are among the most used methods for preparing TiO₂/Ag-based nanocomposites. In particular, the extensively investigated sol-gel synthetic protocols produce Ag NPs by reduction of Ag salt (typically AgNO₃ or AgClO₄) with a suitable reductant, such as ascorbic acid, glucose, sodium borohydride and citrate. Kedziora et al. reported a method for obtaining TiO₂/Ag-based nanocomposites with a control on the amount of Ag. The synthetic procedure was based on two steps: the preparation of the Ag precursor and the sol-gel process. Firstly, a diamminosilver (I) nitrate solution was prepared by adding potassium hydroxide in a silver nitrate solution, resulting in a brown precipitate that was then dissolved in ammonium hydroxide. In the second step, first titanium n-butoxide was added drop wise in acetone, next the diamminosilver (I) and the reducing agent (glucose) were introduced in the reaction vessel obtaining a sol. Afterward, the sol was washed and dried at 80 °C and finally calcinated at 400 °C for 10 h to obtain TiO₂ in anatase phase. This process made it possible to control the amount of Ag NPs nucleating on the TiO₂ surface by simply repeating the process of impregnation with diamminosilver (I) nitrate solution and reduction by glucose. The TEM micrograph of TiO₂/Ag nanostructures in Figure 4 points out the presence of spherical Ag NPs, appearing as high contrast round-shaped spots, in close contact with the surface of the lighter contrast TiO₂ structures [31].

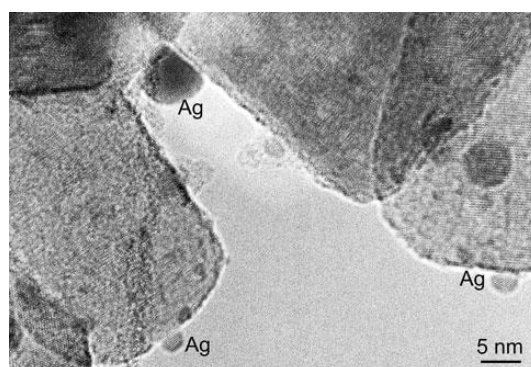


Figure 4. TEM micrograph of TiO₂/Ag nanocomposite. Reprinted from ref. [31], Copyright (2012), with permission from Springer Nature.

Another approach for the preparation of TiO₂/Ag nanocomposites is based on a double step synthesis, consisting of the reduction AgNO₃ in presence of TiO₂ NPs previously prepared by a HT method. In this case, the obtained nanocomposite was deposited on leather for antimicrobial function in the footwear industry. The antimicrobial activity was successfully demonstrated against the bacteria *Pseudomonas aeruginosa* (*P. aeruginosa*), *St. aureus*, and the fungi *Candida albicans* (*C. albicans*) [32]. Moreover, other reports indicated that a post-synthesis treatment carried out at high temperature (up to 500 °C) on TiO₂ NPs before growing Ag NPs resulted in a nanocomposite with a higher crystallinity of the TiO₂ phase in nanocomposite prepared for inactivation of *St. aureus*, *E. coli*, and *Bacillus cereus* (*B. cereus*) [33–35].

Another synthetic method, widely used for the production of TiO₂ nanocomposites for antibacterial applications, relies on photo-reduction of Ag salt by UV radiation onto pre-synthesized TiO₂ NPs. Skorb et al. synthesized TiO₂-based nanocomposites using this method. Firstly, nanostructured TiO₂ was synthesized by means of a sol-gel process, and deposited by spray-coating onto different substrates such as glass microscope slides or glazed ceramic. Afterwards, the deposited material was treated at 200 °C. Subsequently, Ag NPs were deposited on the surface of TiO₂ by dipping the substrate in aqueous solution of AgSO₄ and irradiating with a UV lamp for 10 s. A further step allowed the

preparation of TiO₂/Ag/Ni nanocomposites by electrodeposition of a nickel layer onto a surface of TiO₂/Ag from a Ni(CH₃COO)₂ solution. The antimicrobial activity of the nanocomposite was assessed against *Pseudomonas fluorescens* (*P. fluorescens*) and *Lactococcus lactis* (*Lc. lactis*) [36].

2.2.2. Coupling TiO₂ with Other Metals and Metal Oxides

Current research on TiO₂-based nanomaterials for antibacterial applications is also focusing on valid and cost-effective metal NPs, as alternative to Ag, to merge to TiO₂, possibly characterized also by intrinsic antibacterial properties.

Kaushik et al. developed a TiO₂/Al-based nanocomposite material with antibacterial activity. The synthetic method is essentially a HT process performed in the presence of an Al-based compound. Firstly, titanium (IV) isopropoxide (TTIP) and ethylene diamine were mixed in isopropyl alcohol, next aluminum isopropoxide was added, and finally the solution was transferred to Teflon-lined stainless-steel autoclave and kept at 180 °C for 18 h in oven. The obtained material was found to consist of Al doped TiO₂ NPs, giving Al the twofold role of (i) extending the visible range the wavelengths suitable to activate the photocatalytic properties and (ii) significantly increasing the antibacterial activity with respect to undoped TiO₂. Higher bacterial disinfection activity of the doped samples compared to that of the undoped TiO₂ was observed under visible light irradiation (nearly 80%) as well as in the dark (nearly 20%) against both *St. aureus* and *E. coli* bacteria [37].

Venieri et al. studied the bactericidal activity of TiO₂-based nanostructures doped with Co and Mn for inactivation of *K. pneumoniae* and *E. coli*. They synthesized by sol-gel Mn, Co, and Mn:Co doped TiO₂. Each nanocomposite was synthesized starting from a sol containing both the TiO₂ and the dopant precursor, afterward the pH of the sol was adjusted to pH 7, and finally, the resulting nanocomposite materials were washed with water and thermally treated at 500 °C for 3 h [38–40].

An original approach developed to improve both the antibacterial activity and the photocatalytic properties was based on the use of rare earth metals as dopants for TiO₂ NPs. In particular, Nd is a lanthanide element that attracted a lot of attention, due to its unique optical and magnetic properties, that make it extremely useful for application in optoelectronic and magnetic devices [41]. Nithya et al., produced Nd doped TiO₂ NPs by means of a sol-gel method for inactivation of *E. coli* and *St. aureus*. TTIP and Nd (III) acetate dehydrate were dissolved in isopropyl alcohol at pH 9, afterwards acetic acid was added to complete the hydrolysis reaction. Then, the obtained powder was dried at 120 °C for 2 h and annealed at 600 °C for 3 h [42].

Another effective strategy to increase the antibacterial ability of nanostructured TiO₂ relies on the coupling with a suitable metal oxide semiconductor.

Siwińska-Stefańska et al. synthesized various TiO₂/ZnO binary semiconductor nanocomposites, with different TiO₂:ZnO ratios, by using HT route. In particular, the synthesis of the binary TiO₂/ZnO semiconductor was carried out by mixing TTIP, dissolved in alcohol, with zinc acetate, dissolved in water. The obtained mixture was heated in autoclave at 160 °C. All the synthesized TiO₂/ZnO binary semiconductors showed a well-defined crystalline structure and a high surface area [43]. The nanocomposite demonstrated antibacterial activity against seven different bacteria including *E. coli*, *P. aeruginosa*, *St. aureus*, a methicillin-resistant *St. aureus*, *B. cereus*, *Bacillus licheniformis* (*B. licheniformis*), and anaerobic *Clostridium perfringens* (*C. perfringens*).

Other hybrid nanocomposites, such as TiO₂:In₂O₃, TiO₂:g-C₂N₄, and TiO₂:SiO₂ are currently under investigation due to their promising photoactivity and antibacterial properties [36,44–47]. For instance, TiO₂:In₂O₃ photocatalysts were prepared by sol-gel route by reacting TiCl₄ and In(NO₃)₃ in water and then stabilized by addition of HNO₃. The obtained photocatalyst was able to inactivate *P. fluorescens* and *Lc. lactis* [36]. TiO₂:g-C₂N₄ synthesis involved the growth of TiO₂ nanosheets with (001) facets exposed by a hydrothermal route based on the decomposition of TiO(Bu)₄ in the presence of g-C₂N₄. The TiO₂:g-C₂N₄ nanocomposite was able to inactivate *E. coli* [44]. Mesoporous silica nanospheres functionalized with TiO₂ were prepared in a three-step procedure. The first step was conducted according to a modified Stöber sol-gel method involving the hydrolysis of tetraethyl orthosilicate

(TEOS) in alkaline conditions. In a second step, a mesoporous external layer was deposited on the silica spheres by letting TEOS react in the presence of CTAB (Cetyltrimethylammonium Bromide). Finally, functionalization with TiO₂ was accomplished by means of the reaction of titanium (IV) butoxide at the mesoporous silica nanosphere surface. The photocatalytic antibacterial properties of TiO₂:SiO₂ were investigated against *E. coli* [45].

Other innovative materials recently proposed for their antimicrobial properties are La-doped TiO₂/calcium ferrite/diatomite and TiO₂/chitosan/graphene oxide (GO@CS@TiO₂) [46,47]. The former was prepared by reacting ferric nitrate nonahydrate and calcium nitrate tetrahydrate in the presence of diatomite. In the next step, tetrabutyl orthotitanate and lanthanum nitrate hexahydrate were left to react in the presence of calcium ferrite/diatomite finally leading to La-doped TiO₂/calcium ferrite/diatomite that was able to kill *E. coli* under visible light irradiation [46]. For preparing GO@CS@TiO₂, in brief, GO was dispersed in ultrapure water, then CS was dissolved in acetic acid and added to GO solution obtaining nanometer film. Finally, GO@CS@TiO₂ nanocomposites were prepared by adding colloidal TiO₂ to the GO@CS film. GO@CS@TiO₂ antibacterial properties were investigated against *Aspergillus niger* (*A. niger*) and *Bacillus subtilis* (*B. subtilis*) [47].

Moreover, many reported synthetic protocols propose the modification of commercially available TiO₂ powders. For instance, TiO₂ Aeroxide P25 form Evonik (20% rutile–80% anatase, specific surface area 50 m²/g) was modified with Ag NPs leading to a TiO₂/Ag nanocomposite with strong antibacterial and/or antiviral characteristics [48–51].

Finally, examples of bio-hybrid nanocomposites have also been reported. For instance Kim et al. synthesized TiO₂/glucose oxidase and the presence of glucose oxidase was found to increase the production of ROS under UV-A irradiation for *E. coli* and *B. subtilis* inactivation [52]. Monmaturapoj et al. synthesized TiO₂/hydroxyapatite (HA) combining the antibacterial properties of TiO₂ with the adsorption capability of HA to trap and photocatalytically inactivate H1N1 Influenza A Virus [53]. Li et al. reported on a modified TiO₂ with tannic acid (TA), using a sol gel technique, as the presence of TA was found to enhance interfacial compatibility between TiO₂ and a polyester matrix towards the fabrication of nanofiltration membrane. The TA-modified TiO₂ demonstrated antibacterial properties under UV irradiation against *E. coli* [54].

3. Activity of TiO₂-Based Nanostructured Materials against Bacteria, Fungi, and Virus

This section intends to provide an overview of the antimicrobial photocatalytic activity of the TiO₂ NPs against bacteria, virus, and fungi, critically discussing the numerous parameters affecting the experimental results reported in literature. A large number of experimental variables have been found to affect the efficiency of photocatalytic TiO₂-based NPs in the inactivation of microorganisms. The main parameters considered in the following are structural characteristics of the photocatalytic TiO₂-based materials, morphology of bacteria such as structural, genomic, and physiological features, their metabolism, environmental conditions such as absence/presence of a light source, and environmental stress. Moreover, specific attention will be devoted to the intrinsic antibacterial activity of TiO₂ and TiO₂-based nanocomposite. The antiviral and antifungal activity of TiO₂ nanostructures will be also presented.

As a general scheme, the toxicity mechanism of TiO₂ to pathogenic microorganisms could be summarized as follows (Figure 5): (A) cell damage and lipid peroxidation due to NPs attachments by electrostatic interaction on cell wall, (B) breaking of cytoplasmic flow due to NPs obstruction of nutrients carrier, photocatalytic degradation to (C) biological macromolecular, and (D) intracellular organelles.

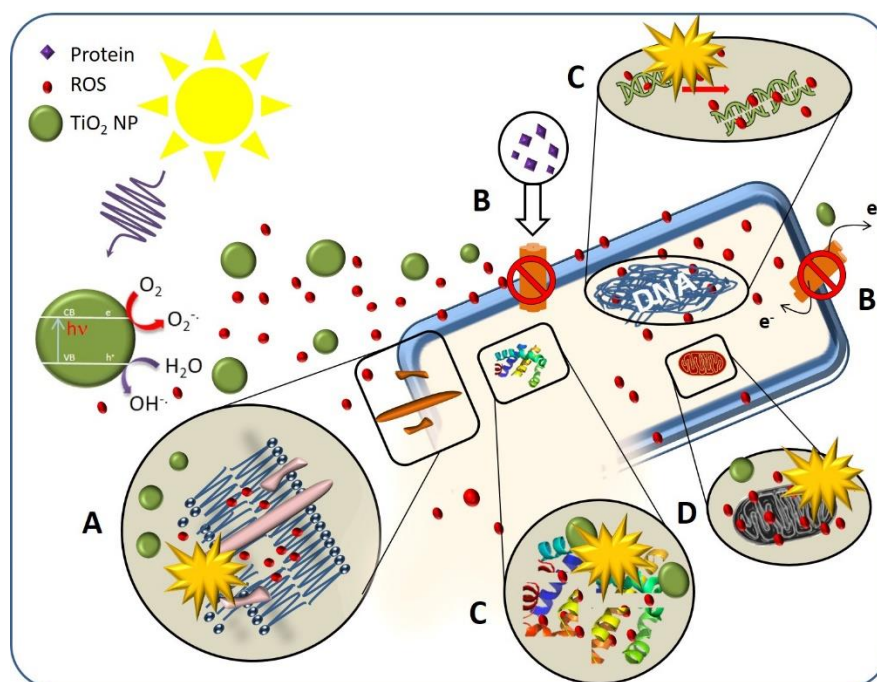


Figure 5. Schematic diagram of TiO₂ NPs toxicity mechanism on the cellular components of the pathogen microorganisms: (A) cell wall, (B) cytoplasmic flow, (C) macromolecular, (D) organelles.

Remarkably, the literature reported experimental results and their interpretation often appear debated and sometimes are in disagreement; therefore, here we aim to illustrate and critically discuss. The criteria identified to select the reported studies are the nanosize regime of the investigated TiO₂ based materials (average sizes in the range 1–100 nm), the analysis of multiple experimental parameters, and the techniques to evaluate the antimicrobial activity of TiO₂ NPs.

3.1. Antibacterial Activity of TiO₂ Nanostructured Materials

3.1.1. Effect of TiO₂ Nanostructure Characteristics

The antibacterial effect of TiO₂ NPs-based nanomaterials was investigated as a function of their chemical-physical characteristics, which include NPs crystalline structure, particle size and shape, doping, and presence of co-catalysts such as metallic NPs and metal oxide NPs. Lin et al. studied the antibacterial effect of five types of TiO₂ NPs, namely pure anatase NPs with average size of 10, 25, and 50 nm, 50 nm rutile NPs, and both anatase and rutile NPs with an average size of 25 nm. The photocatalytic experiments were performed under natural sunlight testing the NPs antibacterial activity against *E. coli* cells. The study was carried out on aqueous solutions at different pHs and ionic strengths. The smallest anatase NPs showed the highest affinity with cell surface in presence of TiO₂ NPs, 50 mg/L, 3 h, and were, thus, found to induce higher oxidative cell damage. Interestingly, pH and ionic strength of the aqueous solution were also found to affect the antibacterial activity of the NPs (Figure 6) [55].

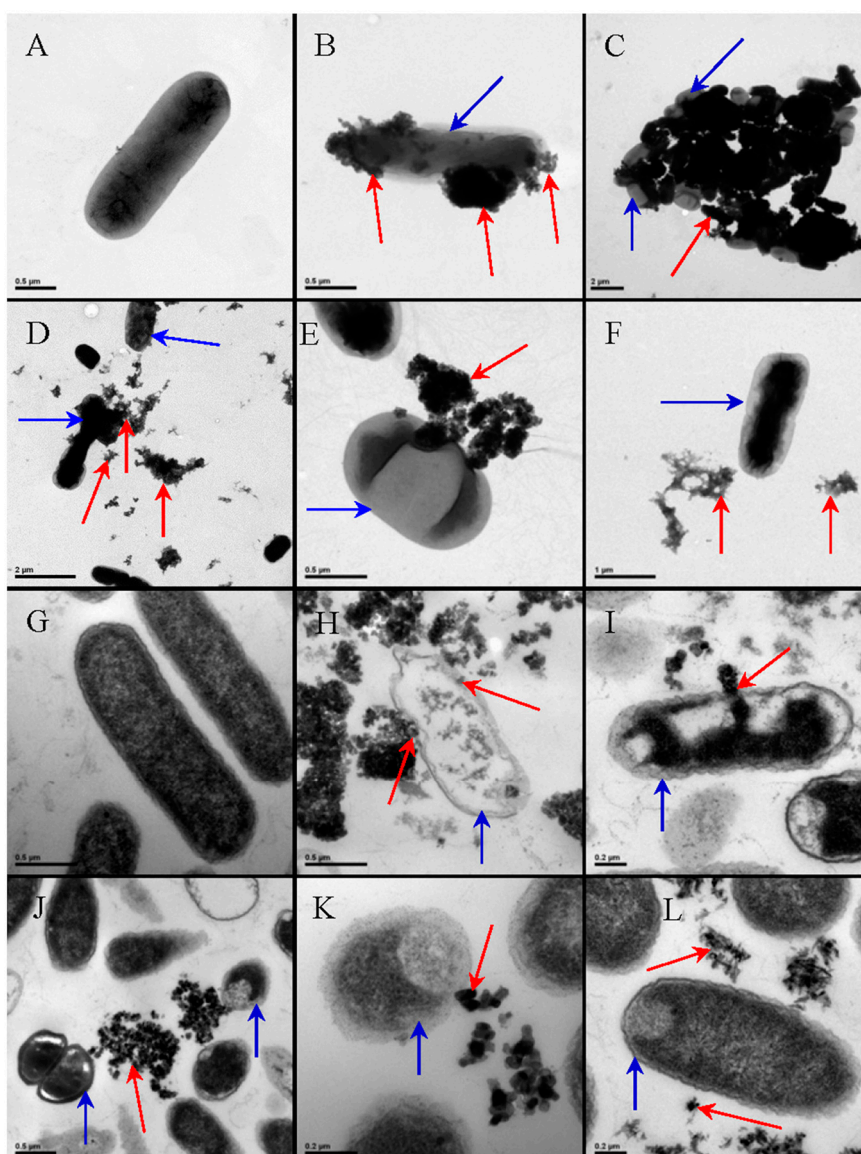


Figure 6. TEM images showed NPs-type-dependent bacterial cell membrane localizations of TiO₂ NPs and the morphological changes of the cell exposed to the NPs: TEM images of the unsliced (A–F) and sliced (G–L) *Escherichia coli* samples: A and G untreated; B and H upon treatment with 10 nm anatase TiO₂ NPs; C and I upon treatment with 25 nm anatase TiO₂ NPs; D and J upon treatment with 50 nm anatase TiO₂ NPs; F and L upon treatment with 50 nm rutile TiO₂ NPs; with all samples having been exposed to natural sunlight. The blue arrows highlight the cells and the red arrows point to the NP aggregates. Reprinted with permission from ref [55].

Shirai et al. compared the antibacterial activity of anatase TiO₂ microparticles (5 μm) and anatase TiO₂ NPs (21 nm). In particular, they studied the extent of antimicrobial effect on switching off the UV light irradiation. The antibacterial activity observed was higher for the 21 nm TiO₂ NPs than the 5 μm TiO₂ microparticles, even 6 h after stopping the UV exposure [56].

In the case of deposited nanostructured TiO₂-based materials, the resulting antibacterial activity may also be affected by the characteristic of the nanostructured coating. Indeed, TiO₂ NPs deposited on polyethylene by HIPMS (high power impulse magnetron sputtering), a pre-treatment of the polyethylene substrate with a RF-plasma (radio frequency-plasma) results in a roughness suitable for improving adhesion of bacterial cells to the substrate, that was found effective in enhancing the efficiency of the photocatalytic TiO₂-assisted bacteria inactivation [57].

Sunada et al. demonstrated the bactericidal activity on *E. coli* and the decomposition ability on its endotoxin (detoxifying activity) of silica thin film (100 nm) modified with TiO₂. Endotoxin is a toxic lipopolysaccharide (LPS) cell wall constituent of Gram-negative bacteria. The authors investigated the effect of TiO₂ film photocatalysts on the concentration of endotoxin and survival ratio of *E. coli*, and found that while the survival ratio of the bacteria decreased either in presence and in absence of the TiO₂ film (due to the germicidal effect of UV light), only in presence of TiO₂ film was there also a decrease of the amount of endotoxin observed, thus highlighting the effect of the TiO₂ photocatalyst on the integrity of the outer membrane of the cells [58].

In addition, modification of TiO₂ nanostructures with metal NPs (Ag, Cu, Ce, Al, In, Mn, and Co), being able to improve the absorption property in the visible of TiO₂ NPs-based nanocomposites, can enhance the efficiency in generation of ROS and, thus, increase the antimicrobial effect. In addition, the metal ions released from the metal NPs, once up taken by cells through their membrane, may interact with functional groups of proteins and nucleic acids, resulting in relevant damage of enzymatic activity, alteration of the cell structure, modification of the normal physiological processes, and, ultimately, in the inactivation of the microorganism [36–38,51,59–61].

Liu et al. studied antibacterial activity of a P/Ag/Ag₂O/Ag₃PO₄/TiO₂ photocatalyst against *E. coli* under LED lamp irradiation. The authors observed a bacterial inactivation of 100% by the composite within 20 min of photocatalytic treatment. On the contrary, under dark conditions, a reduction of *E. coli* was achieved (2-log cycles), attributed to the amount of metal Ag loaded on the composite. The concentration of bacteria remained almost equal in presence of TiO₂ (in both the dark and light conditions). The inactivation process was also investigated by SEM analysis to evaluate cell damage. After 20 min of photocatalytic treatment, changes on the wall surface were observed, namely an increase in roughness or occurrence of holes in the cell wall. After 40 and 90 min, larger pits and holes were observed, and, subsequently the cells were found to be completely decomposed [62].

In general, metal NPs can improve the antibacterial activity both because they are able to enhance photocatalytic performance of TiO₂ and release metal ions, therefore they exert an intrinsic biocidal effect interacting with cells.

3.1.2. Effect of the Cell Membrane Structure

Several types of bacteria were investigated in order to elucidate the antimicrobial activity of TiO₂ NPs and TiO₂ NPs-based nanocomposites. In this perspective, *E. coli*, as a model for Gram-negative bacteria, and *St. aureus* or *P. aeruginosa*, as models for Gram-positive bacteria, have attracted a lot of attention.

The need of investigate the behavior of both Gram-positive and Gram-negative bacteria in response to the photocatalysis-promoted antibacterial properties of TiO₂ NPs arises from the intrinsic differences existing between these two classes of cells in terms of cell membrane structure, that may be responsible for a different interaction with TiO₂-based NPs. In Figure 7, the difference between the cell walls of Gram-positive and -negative bacteria is shown.

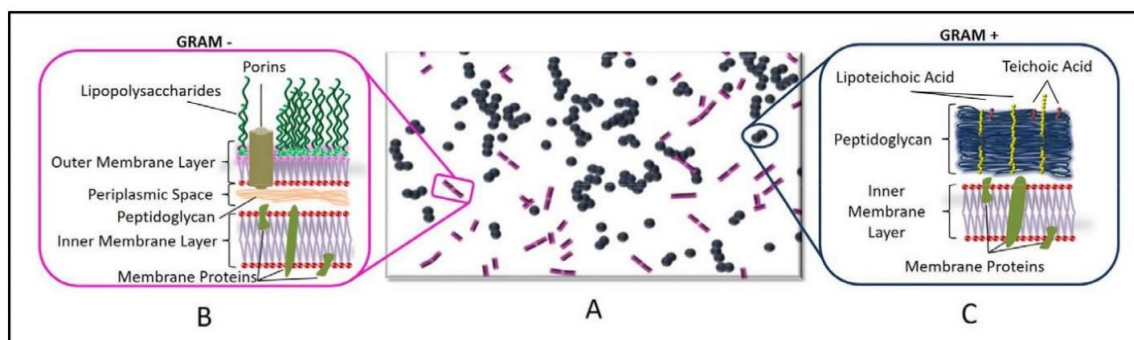


Figure 7. (A) scheme of a Gram staining experiment with a mix of crystal violet stained cocci (Gram-positive bacteria) (blue) and safranin stained bacilli (Gram-negative) (purple) bacteria on a slide and comparison of the cell wall in Gram-negative (B) and -positive (C) bacteria.

For this reason, here, the cell membrane differences between Gram-positive and Gram-negative bacteria will be discussed first, and then relevant studies describing the TiO₂ NPs antibacterial activity as a function of the characteristics of the bacterium membrane structure will be reviewed.

The cell wall of Gram-negative bacteria is characterized by the following features: (i) the presence of an outer membrane (OM) that contains phospholipids in the inner leaflet and glycolipids, mainly lipopolysaccharide (LPS) in the outer leaflet; (ii) a thin peptidoglycan cell wall, consisting of repeated units of disaccharide N-acetyl glucosamine-N-actyl muramic acid, that are cross-linked by pentapeptide side chains; and (iii) a cytoplasmic—or inner—membrane (IM), formed of a phospholipid bilayer.

The intermembrane space between the OM and the IM is characterized by a compartment defined as periplasm, that essentially contains proteins [63]. The OM, thanks to its unique composition, represents a selective barrier, that effectively protects cell from many agents, including detergents and antibiotics, still allowing penetration of specific macromolecules. Furthermore, the OM provides structural stability to the cell [64]. Gram-positive bacteria, instead, lack OM, but possess a 30–100 nm multilayer of peptidoglycans, which is thicker than that present in Gram-negative bacteria, which is a few nm thick [65].

Importantly, the cell wall of Gram-positive bacteria is porous, as the peptidoglycan multilayer can be easily crossed by teichoic acids, formed of glycerol and glucosyl or ribitol phosphate. The teichoic acids are anionic glycopolymers, that provide a high density of negative charge at the surface of the wall, thus making Gram-positive bacteria more prone than Gram-negative bacteria to interacting with positively charged NPs [65].

Several authors considered the ensemble of these features essential to explaining the observed antibacterial activity of TiO₂-based NPs being higher against Gram-positive than Gram-negative bacteria.

Fu et al. studied the effect of photocatalytic activity of TiO₂ NPs at different concentrations under ambient light towards the Gram-negative *E. coli* and the Gram-positive *Bacillus megaterium* (*B. megaterium*). While *E. coli* was found to be inhibited by 5 mM TiO₂ NPs, the highest tested concentration, *B. megaterium* was already inhibited at 1 mM [66].

Page et al. compared the antibacterial effect of TiO₂ and Ag-doped TiO₂ (being TiO₂ in anatase phase in both cases) NPs-based coatings against *E. coli* (Gram-negative) and *St. aureus* and *B. cereus* (Gram-positive bacteria) under UV radiation (254 nm) for 30 min. Both coatings demonstrated photocatalytic and antimicrobial properties; however, the Ag-doped TiO₂ NPs-based coating was found more effective against the Gram-positive bacteria than the bare TiO₂ NPs-based one. Since the peptidoglycan multilayer forming the cell wall, along with the other mentioned components, consists of an open polymers network with peptide bridges, indeed the photogenerated hydroxyl radicals more easily interact and damage the cell wall, as they are not hindered by the surface appendages, that are, instead, present at the *E. coli* surface OM [34].

A similar behavior was observed by Alizadeh Sani et al. The antibacterial activity of a nanocomposite film, composed of whey protein isolate and cellulose nanofibers, 1.0% (*w/w*) TiO₂ and 2.0% (*w/v*) rosemary essential oil, was evaluated and a growth inhibition effect was shown to be higher for Gram-positive bacteria, as *Listeria monocytogenes* (*L. monocytogenes*) and *St. aureus*, than Gram-negative bacteria, as *E. coli*, *Salmonella enterica*, and *P. fluorescens* [67].

Nakano et al. evaluated the microbiocidal activity of photocatalysts for various species (virus, Gram-negative and -positive bacteria). Bactericidal activity of TiO₂ coated glass under UV-A irradiation for 48 h was investigated and the author confirmed that Gram-bacteria cocci (GPC) (*S. aureus* and *Enterococcus* spp.) were promptly inactivated, while Gram-negative cocci (GNC) (*E. coli* and *P. aeruginosa*) were only gradually inactivated [68].

On the contrary, other authors showed that Gram-positive bacteria are more resistant than Gram-negative bacteria. Khezerlou et al. proposed that, due to its composition, the Gram-negative bacteria OM is an attractive target for hydroxyl radicals, produced upon the TiO₂ NPs photoactivation, that can react with the lipidic components of the membrane rather than crossing it. The authors inferred an antibacterial action consisting of two steps: in the first, the OM is compromised, being then involved the cytoplasmic membrane. In the second step, once the OM is breached, the radicals can disrupt cytoplasmic membrane and subsequently induce the cell death [5].

Backhaus et al. (2010) investigated the effect of TiO₂ P25 on two faecal indicator strains, *E. coli* and *Enterococcus faecalis* (*Ent. faecalis*), in real wastewater treatment plant effluents, that is a water matrix with total organic carbon (TOC) values in the range of 8–25 mg_C/L and conductivity in the range 450–750 μS/cm (effluent organic matter, EfOM). By using a UV-A bulb lamp, presenting its highest emission at 365 nm, the authors observed a different response of two types of bacteria to the photocatalytic treatment: *Ent. faecalis* was less sensitive than the *E. coli* to the photocatalytically generated TiO₂ NPs. Such a result was accounted for by the occurrence of the thick peptidoglycan multilayer in Gram-positive bacteria, that might have a higher affinity with EfOM relative to the peptidoglycan layer characterizing Gram-negative bacteria (EfOM protecting *Ent. faecalis* by ROS) [69]. Pal et al. reached the same conclusions upon testing the antibacterial activity of TiO₂ P25 NPs on different species, such as *E. coli* and *P. fluorescens* (as Gram-negative bacteria), and *B. subtilis*, *Microbacterium* spp., *Microbacteriaceae*, and *Paenibacillus* sp. (as Gram-positive bacteria). The authors used an experimental set-up, consisting of an irradiation source (UV-A, 365 nm) incident on the bacterial suspension (in contact with a filter loaded with a defined amount of TiO₂ NPs) by clamping the light source on top of a suitable support, and found that photocatalytic inactivation was more effective against *E. coli* than against *B. subtilis* [70].

Other studies, conversely, observed a negligible difference between two microbial groups. Ripolles-Avila et al. tested two types of commercial TiO₂ NPs, the NM105 (Degussa, Frankfurt, Germany) and the NM101 (Institute for Health and Consumer Protection at the European Commission Joint Research, Ispra, Italy), the former being based on anatase phase 7 nm NPs, while the latter is a mixture of 21 nm anatase and rutile phase (80:20 wt/wt) NPs. The experiments performed to investigate the antibacterial activity of the NM105 and the NM101 were carried out both in the dark and under UV light irradiation (315–400 nm) on *Salmonella enterica* var. Enteritidis, *E. coli*, *St. aureus*, and *B. cereus*. The results indicated that the antibacterial activity was affected by the amount of TiO₂ NPs, both in the dark and under UV-light irradiation. Further, no significant difference, in terms of cell viability, was observed among the different investigated microbes [71]. Analogous results were obtained for TiO₂ NP-coated implants [72] or colloidal dispersions of TiO₂ NPs [73]. In summary, the authors claim that the photocatalytically assisted antibacterial activity of TiO₂ NPs, defined in terms of cell inhibition, does not depend on the features of cell membrane structure. Indeed, Haider et al. used TiO₂ in a self-cleaning transparent coating for windows in outdoors applications, preparing NPs by using TiCl₄ as a precursor, and calcinating at different, increasing temperatures (400 °C, 600 °C, 800 °C and 1000 °C), testing *E. coli* and *P. aeruginosa*. SEM analysis showed that after 2 h of sunlight irradiation, the TiO₂NPs-based coating was effective against both bacteria, as no cells survived [74].

In this case, the authors also concluded that the cell wall structure was not the main parameter involved in bacterium resistance to photocatalysis-promoted antibacterial activity of TiO₂ NPs.

3.1.3. Effect of Bacterial Metabolism

The mechanisms behind cell growth inhibition and bacterial death, induced by the photocatalytic reactions promoted by TiO₂ NPs, have also been analyzed considering two different cell metabolisms. Skorb et al. investigated the effect of the photocatalytic activity of several TiO₂ NPs-based nanocomposites, on two bacteria strains showing a different metabolism: *P. fluorescens*, obligate aerobe, and *Lc. lactis*, facultative anaerobe. The investigated TiO₂ NPs-based nanomaterials, which consisted of thin-films of TiO₂, TiO₂:In₂O₃, TiO₂/Ag, or TiO₂/Ag/Ni deposited on a ceramic substrate, were prepared first by spraying the oxide sols, and then performing silver photo-deposition and electroless nickel deposition in order to convey antibacterial properties. According to the results, the differences between *P. fluorescens* and *Lc. lactis* in terms of bacteria inactivation rate could be associated to the morphologies of cell envelopes and to the resistance of OM to radicals generated from the photocatalytic reactions [36]. In particular, *P. fluorescens* uses the oxidative phosphorylation to store energy required for cell respiratory functions. Therefore, for this type of cell, the increase of ion permeability of the cytoplasmic membrane, due to the damage induced by ROS, causes the loss of the proton gradient and consequently inhibits bacteria respiratory function. *Lc. lactis* (facultative anaerobe), instead, stores energy thanks to other metabolic process (such as lactic acid fermentation). For this reason, the damage on the cytoplasmic membrane detected in *Lc. lactis* was scarcely relevant [36].

3.1.4. Effect of Physiological State of Bacteria Cell and Environmental Stress

Rincón et al. claimed that in photocatalytic bacteria inactivation experiments, the rate of cell inactivation can be affected by the bacterial growth state (exponential or stationary phase) as well as by generation state of the culture. Indeed, *E. coli* cells, collected during the exponential step, were inactivated in a shorter timeframe (1 h) with respect to the same cells collected during the growth stationary phase, that, instead, required 2.5 h to be completely inactivated in presence of P25 TiO₂ NPs under simulated sunlight irradiation. Moreover, *E. coli* cells from the third generation were found more resistant compared to those from the seventh generation.

The authors suggested that the performance of the TiO₂ assisted photocatalytic inactivation was influenced by physiological state and generation of the bacteria [75]. In detail, environmental stress was thought able to induce expression of genes involved in the synthesis of a specific set of proteins, that have been found responsible for mutations in the following generations. In addition, the stationary phase response to environmental changes induces the synthesis of the proteins that convey to *E. coli* resistance to several types of stress (i.e., heat shock, oxidation—UV light—, hyperosmolarity, and acidity). During the stationary phase, the expression of *rpoS* is also induced, which encodes a regulator for expression of genes [76,77], such as those involved in the protection against oxidants (e.g., catalase) and in the reparation of oxidative damage (e.g., exonuclease III) [78,79].

Another important factor is represented by the ability of bacteria to resist to environmental stress. Upon environmental stress, the bacteria can activate several mechanisms of defence, in order to limit the damage. Indeed, it is well known that there are specific enzymatic systems able to eliminate ROS. In bacteria such as *St. aureus* or *Staphylococcus pyogenes* (*St. pyogenes*), anti-ROS mechanisms, often associated to pathogen virulence, were identified [80,81]. Furthermore, bacteria are able to produce a biofilm that prevents the penetration of NPs into the cell membrane, thus hampering their antibacterial functions.

Interestingly, in TiO₂ NPs-assisted photocatalytic reactions, the concentration of ROS physiologically produced in presence of bacteria is another important parameter to be taken into account when considering cell damage [82]. Bonnet et al. investigated Gram-positive bacteria (*St. aureus* and *Lactobacillus casei rhamnosus*, *Lb. casei rhamnosus*) and Gram-negative bacteria (two different strains of *E. coli*) in contact with anatase TiO₂ NPs under UV light irradiation. In particular, after 30 min,

St. aureus was found to be more resistant than the other bacteria under the investigated experimental conditions. Such evidence was explained in terms of the detoxification ability of the catalase activity, which is typical of this bacterium, and that was exerted in presence of TiO₂ NPs. Indeed, catalase is able to trigger the oxidative stress-related mechanisms against endogenous ROS (such as H₂O₂), metabolites naturally produced by these cells, that consequently need to remove them by activating detoxification mechanisms; the same mechanisms can thus act against TiO₂ NPs-induced ROS [83]. These features, therefore, suggest that the resistance may be species-dependent.

3.1.5. Intrinsic Antibacterial Activity of TiO₂

The intrinsic antibacterial activity of TiO₂ NPs in the dark is an extremely controversial and debated issue, that, in fact, often hinders the use of TiO₂ NPs in any kind of application that does not allow light irradiation. Erdem and other authors [84,85] confirmed that different types of TiO₂ NPs were able to promote a short-term bacteria inactivation, even in the dark. In detail, in this case a possible killing mechanism is assumed to mainly involve the direct interaction between TiO₂ NPs and bacterial membrane. Indeed, the OM of Gram-negative bacteria (especially in *E. coli*) contains porins, which are membrane proteins acting as pores (1.5–2 nm in diameter) enabling diffusion of molecules in the cytoplasmic compartment. When the TiO₂ NPs and bacteria are in close contact, NPs may obstruct such pores, thus hindering the diffusion channels, preventing nutrition uptake, finally inducing cell death.

The close contact between TiO₂ NPs and *E. coli* OM was identified by Kiwi et al. as an essential condition, responsible for the intrinsic antibacterial activity of TiO₂ NPs in the dark. Such a conclusion was reached by monitoring *E. coli* inactivation experiments by TEM microscopy. Indeed, TEM micrographs, collected at different inactivation times, pointed out that, at suitable TiO₂ NPs amounts and at a pH close to its isoelectric point, aggregates of TiO₂ NPs migrate towards the OM of *E. coli*, where they accumulate due to electrostatic interactions, finally leading to extensive damage of the OM and therefore to the loss of *E. coli* cultivability [86–88]. Ripolles-Avila et al. investigated the antibacterial activity of TiO₂ NPs both in the dark and under UV-light irradiation. The test performed against both Gram-negative and -positive bacteria demonstrated an intrinsic bactericidal activity of TiO₂ NPs, since no significant differences, in terms of cell inactivation rate was observed with or without irradiation [71]. However, the presence of NPs was demonstrated to affect the bacteria growth, especially at low cell population density [89].

The antibacterial effect of P25 TiO₂ NPs was also investigated by Carré et al. (2014) against *E. coli*, specifically considering lipid peroxidation phenomena and performing a proteomic analysis. The extent of lipid peroxidation, through the thiobarbituric acid (TBA) assay, was found to significantly increase both in the dark and under UV-A-light irradiation, after 60 min exposure to TiO₂ P25 at a concentration of 0.4 g/L. The proteome of bacteria was investigated by means of electrophoresis (2-DE), that is able to identify the extent of protein damage under different experimental conditions, namely at two distinct TiO₂ NPs concentration (0.1 or 0.4 g/L) with and without UV-A irradiation, and evaluated against two control tests performed without catalyst, with and without irradiation, for 30 min. In particular, in presence of TiO₂ NPs, both in the dark and under UV-A irradiation, OM proteins suffered most alterations, probably due to the direct contact with TiO₂ NPs [90]. On the other hand, several authors observed that TiO₂ NPs in the dark did not exhibit toxic effects on bacteria [89,91].

Another possible interesting explanation for the intrinsic, non-photoinduced, antibacterial activity of TiO₂, though non-nanostructured in nature, was reported by Lifan et al. who demonstrated that the germicidal activity of their sol-gel synthesized TiO₂ NPs was not UV-induced, under the investigated experimental conditions, being, instead, directly related to the wettability property of TiO₂ NPs [50]. The surface of TiO₂ NPs was found characterized by both hydrophobic and hydrophilic areas, the latter causing a deformation of the cells they get in contact with. In fact, the cell lost its rounded shape and flattened. This phenomenon was expected to build up pressure in the cell, which resulted in a burst of the cell and release of the contents.

3.2. Virus Inactivation

Viruses are ubiquitous biological entities much smaller than bacteria (0.01–0.03 μ). However, they are not independent organisms, presenting independent metabolic activities. Indeed, they need to infect a host for their reproduction. Viruses usually involved in waterborne disease outbreak are noroviruses (NoV), hepatitis A virus (HAV), hepatitis E virus (HEV), adenovirus (AdV), astrovirus, enteroviruses (EV), and rotavirus (RV). In particular, enteric viruses have high infectious capacity, that is, a low amount of viruses is sufficient to induce an infection (i.e., <10 – 10^3 virus particles) [92]. Viruses can often be detected on surfaces, because the structure of their capsid provides them environmental stability. Surfaces can play a crucial role in the spread of microorganisms, especially in a nosocomial environment, where the presence of viruses on the surfaces of equipment, furniture, and medical devices, as well as wall surfaces, represent a potential risk for patients and operators [93]. Moreover, viruses are also widespread in public spaces, including offices, canteens, and kindergartens. Once a surface is contaminated, it immediately becomes a contamination source for individuals and, consequently, other objects. For instance, in the case of NoV, it has been observed that it is possible to transmit the virus to up to seven different surfaces by simply handling contaminated objects [94]. Finally, viruses persist on the surfaces for an extremely long timeframe, ranging from 2–3 h (for HAV and coronavirus) to 20 weeks (for vaccinia virus) [95], thus being extremely critical for infection propagation.

Recently, the photocatalysis-promoted antiviral activity of TiO₂ NPs has been extensively investigated with the aim of limiting the spread of viruses, given that the antiviral behavior of TiO₂ NPs is less documented than the antibacterial characteristics. In this regard, the most investigated models of viruses or phages include bacteriophage MS2 [96–98], *t4* [99,100], *Qb* [101], λ [102], *phi-X174* and *fr* [103], NoV [94], herpes simplex virus-1 (HSV-1) [104], human influenza A virus [105]; H1N1 influenza A virus [53], avian influenza virus A/h5N2 [106], and influenza virus strain A/Aichi/2/68 (H3N2) [107]. Remarkably, these models of virus/phage are interesting both from an environmental and health point of view.

When phage is used as a model, often the system involves the infection of a bacterium by a specific phage, such as the commonly investigated *E. coli*.

Generally, most experimental studies were carried out in aqueous solution, investigating virus exposure to TiO₂ NPs, both in the dark and under different irradiation conditions, given that the virus is able to interact with the TiO₂ NPs [96–99,102,108] both dispersed and immobilized on suitable substrate.

Many reports demonstrated how the environmental conditions can affect viral inhibition by photocatalytic TiO₂ NPs. For example, Syngouna et al. showed that the presence of quartz sand altered the antiviral efficiency of TiO₂ NPs against the bacteriophage MS2-*E. coli* both under sunlight irradiation and in the dark, resulting in a higher virus inactivation rate in absence of quartz sand. However, at higher virus concentration, the excessive viral density was demonstrated to inhibit the antiviral activity [97] of TiO₂ NPs. Zheng et al. obtained analogous results and assumed that a high viral density saturates the reactions sites on the photocatalyst surface, thus leading to limited ROS production [108]. Syngouna et al. (2017) also tested the antiviral activity of TiO₂ NPs in double distilled water (ddH₂O) solution and in phosphate buffered saline solution (PBS), demonstrating that a higher MS2-*E. coli* inactivation could be obtained in ddH₂O rather than PBS solution. This is most likely because the PBS induces MS2 aggregation, due to the ability of the proteins of MS2 to bind of phosphate ions, given that virus aggregation is known to reduce the efficiency of photocatalytic TiO₂ NPs in MS2 virus inactivation [97]. Different characteristics of the aqueous medium may affect the photocatalytic antiviral activity, including temperature [102], pH [98], and presence of inorganic ions [91]. The effect of temperature on the Cu-TiO₂ nanofiber-assisted removal of bacteriophage f2 under visible light irradiation was shown by Zheng et al. [108]. In particular, a relatively low temperature (15 °C) was found to negatively affect the virus removal rate, In fact, although in the first 30 min, the rate at 15 °C was the highest under experimental conditions, after 90 min it decreased significantly, resulting, instead, in the removal efficiency at 25° and 35 °C being much higher. Koizumi et al. observed that

inactivation rate of the phage MS2 in presence of TiO₂ P25 irradiated by black light fluorescent lamp was influenced by pH, given that it was higher at pH 6 than at pH 3.0 and 10.0 [98].

Moreover, the turbidity of water matrices, affecting the absorption of incident light [109], can reduce the photocatalytic efficiency, leading to a decrease of ROS production. Therefore, a suitable design of photocatalysis experiments needs to take into account the penetration depth of the wavelengths selected for the experiments [109]. For instance, in distilled water, 254 nm radiation loses 30% of its intensity already 40 cm below the solution surface.

Ishiguro et al. (2011) investigated the antiviral effect of TiO₂-NPs (anatase) coated glass plates on bacteriophage Q β and T4 (host *E. coli*), as representative models of RNA and DNA viruses, respectively. The effect of UV light intensity (0.1 and 0.25 mW/cm² UV-A) and irradiation time (1, 2, 4, 8, and 24 h) were investigated and both bacteriophages became inactivated when in contact with the TiO₂-coated glass irradiated with 0.001 mW/cm² UV-A light. However, the inactivation of T4 was lower than that of Q β when exposed to UV-A at an intensity lower than 0.01 mW/cm², for 4 and 8 h. Although the photocatalysis was sufficient to inactivate both viruses, these results suggest that the ratio of inactivation varies according to the type of virus [100].

Gerrity et al. compared the disinfection potential of TiO₂ P25 NPs irradiated by a low-pressure UV-lamp with respect to a UV-light source, using bacteriophage PRD1, MS2, phi-X174 and *fr*, which are characterized by different physical and molecular features (size, nucleic acid composition and topology, genome length, mode of infection). The authors observed that in order to reach an inactivation rate of 4-log, a different UV intensity reduction, namely 19%, 15%, and 6%, was required for PRD1, MS2, and phi-X174, respectively. Interestingly *fr* was found to be UV-resistant [103]. The detected differences in inactivation efficiency were associated to structural differences among the investigated viruses.

Nakano et al. tested antiviral activity of TiO₂ coated glass on influenza virus (IFV) and feline calicivirus (FCV), according to the same procedure reported in Section 3.1.2. The authors found that IFV was inactivated by photocatalysts significantly faster than FCV, thus indicating that the virucidal effect of the photocatalyst may depend on the presence of a viral envelope, given that IFV is an enveloped virus, while FCV a non-enveloped virus [68].

The same authors studied the human influenza A virus as a viral model for the TiO₂ NPs-assisted photocatalysis Experiments [105], carried out by tuning irradiation time and UV-A lamp intensity in the range of 0.001–1.0 mW/cm. After 8 h incubation, a reduction of approximately 3-log was observed by using low intensity UV-A-light (0.01 mW/cm). A decrease of viral inactivation was observed with the decrease of UV-A light intensity. After 8 h incubation, a reduction of approximately 3-log was observed by using low intensity UV-A-light (0.01 mW/cm²). However, even with an irradiation intensity of 0.001 mW/cm², the TiO₂-coated glass effectively inactivated the virus after 16 h of incubation, with a reduction of 4-log. At high UV-intensity (1.0 mW/cm²), a much faster viral inactivation was found (3-log after 4 h). Therefore, irradiation intensity and time affect the inactivation efficiency of the prepared TiO₂-coated glass against influenza virus.

The mechanisms of virus inactivation by TiO₂ NPs-assisted photocatalysis are a debated topic. Some authors suggest that ROS induce the capsid protein degradation, as demonstrated through different techniques (qPCR; sodium dodecyl sulphate–polycrylamide gel electrophoresis, SDS-page; etc) [97,100,103,110], while others (Nakano et al. (2012)) indicated, on the basis of real-time reverse-transcription PCR (RT-PCR) and SDS-page, RNA degradation only after the destruction of viral proteins involved in binding, therefore the infectability decreased [105]. Hajkova et al. demonstrated the photocatalytic effect of thin TiO₂ film in presence of UV-A light on the virus HSV-1. The experimental results proved that interaction of the virus with the photocatalytic surface caused significant changes in the virus structure, for instance, inducing the loss of viral glycoprotein, gC, responsible for the first attack of the virus on the target cell, thus resulting in the virus' inability to attack host cells [104].

The antigens, present in the capsid, were also considered to elucidate the effect of TiO₂ NPs. For example, the degradation of HBsAg, hepatitis B surface antigen, typical of hepatitis B virus (HBV) was evaluated in assessing its role in the photocatalytic antiviral activity of TiO₂ NPs. The degradation of

the HbsAg antigen was found affected by the exposure time, amount of photocatalyst, and light-source. The inactivation of the antigen occurred after 12 h exposure. HbsAg degradation extent increased as the TiO₂ concentration increased. In addition, the effect of the light source on the photodestruction level of HbsAg was also shown, following the order UV lamp > mercury lamp > natural light > weak light (i.e., in the dark while not optically filtered) [110].

Furthermore, TiO₂-NPs-based nanocomposites showed promising results for photocatalytic inactivation of viruses. A palladium-modified nitrogen-doped titanium oxide (TiON/PdO) photocatalytic fiber was effectively used for the disinfection of the coliphage MS2 with its host (*E. coli*) by Li et al. In the dark, a significant virus adsorption was measured (95.4–96.7%), while, after 1 h irradiation with visible light ($\lambda > 400$ nm) a virus removal of 94.5–98.2% was achieved [96]. Monmaturapoj et al. showed the effect of hydroxyapatite-titania composite (HAP/TiO₂) on H1N1, investigating the role played by nanocomposite amount, virus concentration, and UV-light irradiation time. An H1N1 photocatalytic inhibition efficiency dependent on the amount of photocatalyst was observed. In particular, no virus inhibition was measured for a HAP/TiO₂ concentration higher than 0.5 mg/mL. The HAP/TiO₂ nanocomposite was able to merge two functions in one nanomaterial: the virus adsorption on the photocatalyst surface, promoted by HAP, and ROS production, induced by UV light irradiation of TiO₂ [53]. Finally, SiO₂-TiO₂ NPs and Ag-doped TiO₂ NPs (nAg/TiO₂) should be also mentioned for their high photocatalytic inactivation rates against the bacteriophage MS2 [49,111].

The current pandemic situation, related to the spreading of the SARS-CoV-2 virus, stimulated the researchers towards the understanding of its ability to persist on the surfaces [112], and towards the investigation of original and reliable solutions suitable for limiting the spread of SARS-CoV-2. Recently, Khaiboullina et al. (2020) explored the photocatalytic properties of nanosized TiO₂ NPs, deposited on glass coverslips, under UV radiation, against the inactivation of HCoV-NL63, namely a human coronavirus belonging to the family of α -coronaviruses, which also includes SARS-CoV-2 [113]. The experimental results highlighted the virucidal efficacy of photoactive TiO₂ NPs, as examined by quantitative RT-PCR and virus culture assays.

3.3. Fungi Inactivation

The scientific community has also started to intensively investigate antifungal properties of photocatalytic TiO₂ NPs. In spite of the low number of reports on the antifungal photocatalytic activity of TiO₂ nanostructured materials, increasing attention can be noticed, motivated by the ability of fungi (filamentous forms and yeasts) to produce dangerous mycotoxins in the water. Further, fungi and their spores are often present on surfaces, including foodstuff, as well as in indoor and outdoor environments. Fungi infect a host, behaving as parasites or by causing the decay of organic matter.

Fungi typically used as a model substrate to investigate antifungal propriety of TiO₂ NPs are: *C. albicans*, *Saccharomyces cerevisiae* (*S. cerevisiae*) [114], *Penicillium expansum* (*P. expansum*) [115], *Aspergillus fumigatus* (*A. fumigatus*) [82], *A. niger* [114,116], *Fusarium* sp. [116–118], and *Penicillium chrysogenum* (*P. chrysogenum*) [119].

Compared to bacteria and viruses, fungi survive in much more stressful conditions (high saline/sugar concentration, high osmotic pressure and extreme pH). They have a complex structure and can show several morphologies. Indeed, molds are multicellular filaments, while yeasts are unicellular organisms. Fungi have a robust cell wall, mainly formed of chitin, with lamellar morphology, given that each layer is made up of fibrils crossing each other in different directions. Fungi (filamentous and yeast species, conidia, hyphae) showed different responses to the TiO₂ NPs treatment. Rodrigues-Silva et al. tested the effect, of TiO₂-assisted photocatalysis on spores of *A. fumigatus*, both in water and air. After 60 min UV-A-irradiation, the inactivation of spores was observed, while after 180 min the complete inhibition of the microorganism's growth was detected. They pointed out a direct correlation between the TiO₂ NPs loading and the disinfection efficiency in aqueous media, as the higher the photocatalyst loading, the greater the photoinduced inactivation of fungi [82].

Seven et al. (2004) studied the effect of TiO₂ P25 (0.01 mg/mL) on different organisms (bacteria and fungi, such as filamentous and yeast species) using a sodium lamp as a light source. The TiO₂ disinfection ability was tested on different bacteria, in particular *C. albicans* and *A. niger*. *C. albicans* were inhibited after 120 min, whereas no inhibition was observed for *A. niger* even if the irradiation time was extended up to 240 min [114]. Furthermore, Polo-Lopez et al. (2010) tested TiO₂ P25 NPs on *Fusarium* sp and observed a greater resistance of the chlamydo spores, followed by macroconidia and microconidia, due to their extremely complex structure, which is able to hinder the penetration of ROS [120]. The resistance to TiO₂ assisted deactivation of spores belonging *C. albicans* and *A. niger* was also reported [116,121,122].

Maneerat et al. (2006) tested the photocatalytic activity of TiO₂ powder and of a TiO₂ NPs-based coating on a plastic film, in vitro and on fruit rot (tomato and apple) in presence of UV-A source against *P. expansum*. [115] The severity of fruit rot was estimated by visual appearance and scored from 0 to 4 (0 = no decay; 4 = decay covering more than 50% of the whole fruit area). No inhibition effect on fungi growth was observed for the TiO₂ powder in the dark (control), while in presence of TiO₂ NPs under UV-A light irradiation, the growth decreased relative to the control experiment. Moreover, the TiO₂ NPs-based coating on the plastic film revealed *P. expansum* inhibition higher than in the control experiment (scores 1.9 vs. 3.2). Kuhn and co-workers (2003) investigated the damage induced by TiO₂ NPs under UV-A light irradiation by means of SEM analysis, highlighting a grainy and partially destroyed cell surface [123].

The differences among the various species of fungi in terms of structural features have been found reflected in their response to interaction with ROS generated by photocatalysis-assisted TiO₂. The main difference among spores is in the wall as unicellular microconidia without septa and larger pluricellular macroconidia with septa both have a single cell wall, while chlamydo spores exhibit a double thick wall [124]. Such a difference explains the highest resistance of chlamydo spores (followed by macroconidia and microconidia) to photocatalysis [112].

Furthermore, the nature of the investigation medium also contributed to inactivation of spores in presence of TiO₂ and solar irradiation. Indeed inactivation rate values in distilled water were found higher than those detected in well water, most likely due to the presence of carbonates/bicarbonates [116]. Indeed, inorganic salt was reported to decrease the TiO₂ photocatalytic efficiency [125,126], mainly because of the formation of an inorganic layer at the TiO₂ surface.

3.4. General Considerations

In spite of the great attention attracted by the antimicrobial properties of TiO₂ nanostructured materials, the experimental evidence and the interpretation of the experimental results reported in the different studies, as also seen in this review, are often debated and, somehow, controversial.

Many of the discrepancies in the results can be ascribed to the diversity of methods used to investigate the photocatalytic disinfection. In order to highlight this variety of conditions, the experimental photocatalytic and operational parameters, including details of the set-up, for bacterial, viral, and fungal disinfection tests are collected in Tables 1–3, respectively. Furthermore, as summarised in Figure 8, TiO₂ NP characteristics (Figure 8A) affect the photocatalytic efficiency while the microorganism structure (Figure 8C), its metabolism (Figure 8D), and local environment adopted for its growth (Figure 8E) strongly affect the response of the microorganism to photocatalytic inactivation (Figure 8B).

Table 1. Summary of the experimental conditions reported in the literature for TiO₂-based nanomaterials photocatalyzed bacterial disinfection.

Photocatalyst	Phase/Size	Experimental Parameters			Bacteria		Disinfection Efficiency	Ref.
		Catalyst Loading	Light Source/Light Flux	Exposure Time	Strain	Cell Density		
TiO ₂	66 and 950, nm, 44 μm anatase/10–50 nm;	10–5000 ppm	Sunlight	360 min	<i>E. coli</i> , <i>B. subtilis</i>	OD ₆₀₀ = 0.002	45–75%	[85]
TiO ₂ NPs	rutile/25 nm; anatase-rutile/25 nm	10–500 mg/L	Natural light	180 min	<i>E. coli</i>	OD ₆₀₀ = 1	0–100%	[55]
TiO ₂	anatase/21 nm, 5 μm	15 mg	BLB ^o /27W	60, 180, 360 min	<i>Porphyromonas gingivalis</i>	OD ₆₆₀ = 0.2	0–80%	[56]
TiO ₂ NPs	n.a.	0.01–5 mM	Room light	n.a.	<i>B. megaterium</i> , <i>E. coli</i>	OD ₆₀₀ = 0.8–1	Size of inhibition zone (disk agar diffusion method)	[66]
TiO ₂ P25	20 nm	0.05 g/L	UV-A bulb lamp/125W	120–280 min	<i>Enterococcus faecalis</i> , <i>E. coli</i> <i>Salmonella entericavar.</i> <i>Enteridis</i> , <i>E. coli</i> , <i>St aureus</i> , <i>B. cereus</i> , <i>Lb casei</i> , <i>Lb delbrueckii</i> subsp. <i>bulgaricus</i> , <i>Lb lactis</i> subsp. <i>lactis</i> , <i>Lb acidophilus</i>	6 log CFU/mL	t _{max} ^o = 15.4–204 min	[69]
TiO ₂ NPs	anatase/7 nm; anatase-rutile (80:20 wt/wt) 21 nm	0.78–100 μg/mL	UV light (315–400 nm)/n.a.	24 h	<i>P. aeruginosa</i> , <i>St. aureus</i>	7 log CFU/mL	OD ₆₅₀ = 0–0.8	[71]
TiO ₂ NPs	anatase-rutile/8–17 nm	1 mg/cm ²	Sunlight irradiation	120 min	<i>E. coli</i> , coliforms, <i>Enterococcus</i> spp. <i>St. aureus</i> , <i>Lb casei</i> <i>rhamnosus</i> , <i>E. coli</i>	7 log CFU/mL	100%	[74]
TiO ₂ P25	n.a.	0.25–1 g/L	Solar irradiation	180 min	<i>E. coli</i> , coliforms, <i>Enterococcus</i> spp. <i>St. aureus</i> , <i>Lb casei</i> <i>rhamnosus</i> , <i>E. coli</i>	8 log CFU/mL	Eliminated in 0.5–2.5 h	[75]
TiO ₂ NPs	8 nm	50–1200 mg/L	UV lamp/48W	30 min	<i>E. coli</i>	6 log CFU/mL	Mortality rate = 80–100%	[83]
TiO ₂ P25	20 nm	0.1–0.8 g/L	BLB/40W	30–60 min	<i>E. coli</i>	6 log CFU/mL	Log ₁₀ (C/C ₀) ^o = −0.3–−3	[90]
TiO ₂ film	100 nm	n.a.	BLB/15W	4 h	<i>E. coli</i>	2 × 10 ⁵ CFU/mL	Survival ratio = 50%	[58]
TiO ₂ -coated glass	200 nm	n.a.	BLB/0.1 mW/cm ²	0–16 h	<i>E. coli</i> , <i>Serratia marcescens</i> , <i>K. pneumoniae</i> , <i>Acin. baumannii</i> , <i>P. aeruginosa</i> , <i>St. aureus</i> , <i>Enterococcus</i> spp., <i>Str. pneumoniae</i>	10 ⁷ CFU/mL	10 ¹ –10 ⁵ CFU/mL	[68]
PE ^o -TiO ₂ film	n.a.	0.031–0.051 TiO ₂ wt%/wt PE	Solar simulator/50W	300 min	<i>E. coli</i>	6 log CFU/mL	Eliminated in 55–260 min	[57]
TiO ₂ ; Ag- TiO ₂ film	n.a.	n.a.	UV lamp (254 nm)/n.a.	30 min	<i>St. aureus</i> , <i>E. coli</i> , <i>B. cereus</i>	6 log CFU/mL	4.5 log CFU/ml	[34]
TiO ₂ NP TiO ₂ -In ₂ O ₃	anatase	n.a.	Hg lamp (filter 300–400 nm)/125W	10 min	<i>P. fluorescens</i> , <i>Lb lactis</i> spp. <i>lactis</i>	n.a.	1–3 log CFU/ml	[36]
TiO ₂ /AgTiO ₂ /Ag/Ni P/Ag/Ag ₂ O/Ag ₃ PO ₄ /TiO ₂	n.a.	0.5 g/L	LED lamp/<0.3W	20 min	<i>E. coli</i>	10 ⁷ CFU/mL	0–10 ⁷ CFU/mL	[62]

^oOD = optical density; BLB = black light blue lamps; PE = polyethylene; CFU = colony-forming units; t_{max}^x = time at which the maximum inactivation rate (V_{max}) is achieved; log₁₀(C/C₀) = the logarithm of reduction, where C₀ is the concentration of control live bacteria without TiO₂ in the dark (CFU/mL), and C is the concentration of live bacteria for other conditions (CFU/mL).

Table 2. Summary of the experimental conditions reported in the literature for TiO₂ and TiO₂-based nanocomposite photocatalyzed viral disinfection.

Photocatalyst	Phase/Size	Experimental Parameters			Virus		Disinfection Efficiency	Ref.
		Catalyst Loading (mg/L)	Light Source/Light Flux	Exposure Time	Strain	Cell Density		
TiO ₂ P25	anatase/25 nm	n.a.	Ambient light/n.a.	0–30 days	Phage MS2	3–8 log PFU°/ml	Log ₁₀ (C/C ₀) = 0.02–0.05	[97]
TiO ₂ P25	anatase/rutile	n.a.	Low-pressure UV light/n.a.	n.a.	Bacteriophage PRD1, MS2, phi-X174, fr	n.a.	4 log CFU/ml	[103]
TiO ₂	n.a.	n.a.	BLB°/1 mW	8 h	Human influenza A	4.0 × 10 ⁸ PFU/ml	Complete in 5 min	[105]
TiO ₂ -coated glass	200 nm	n.a.	BLB/0.1 mW/cm ²	0–16 h	Influenza virus, feline calicivirus	10 ⁷ PFU/mL	10 ² –10 ⁶ PFU/mL	[68]
Cu-TiO ₂ nanofibers	n.a.	25–150	Xe lamp/0–130 mW/cm ²	240 min	Bacteriophage f2	4 log PFU/ml	Q = 1–5.5	[108]
Cu ₂ ⁺ /TiO ₂ -coated cordierite	anatase	n.a.	FL20 BLB (λ = 351 nm)/0.001–0.1 mW/cm ²	24 h	Qβ and T4 bacteriophage	n.a.	Complete in 4–8 h	[101]
nAg/TiO ₂	anatase	100	UV-A lamp/8W	2 min	Phage MS2	3.0 × 10 ⁷ PFU/mL	Inactivation rate = 1.6–6 log	[49]
TiON/PdO	n.a.	100	Xe arc lam/1000W	120 min	Phage MS2	3.0 × 10 ⁸ PFU/mL	1.5 log in 60 min	[96]
HA°/TiO ₂	n.a.	0.125–0.5	UV light/n.a.	180 min	Influenza virus H1N1	10 ⁷ TCID ₅₀ °/mL	2 log TCID ₅₀ /mL	[53]
SiO ₂ -TiO ₂	25 nm	1–102.6	UV-A/8 W	2 min	Phage MS2	10 ⁴ –10 ¹⁰ PFU/mL	5 log in 1.8 min	[111]

°PFU = plaque-forming unit; log₁₀(C/C₀) = the logarithm of reduction, where C₀ is the concentration of control live bacteria without TiO₂ in the dark (CFU/mL), and C is the concentration of live bacteria for other conditions (CFU/mL); BLB = black light blue lamps; Q = microorganism removal efficiency; CFU = colony-forming units; HA = hydroxyapatite; TCID₅₀ = fifty-percent-tissue-culture-infective-dose.

Table 3. Summary of the experimental conditions reported in literature for TiO₂-based nanomaterials photocatalyzed fungal disinfection.

Photocatalyst	Phase/Size	Experimental Parameters			Fungi		Disinfection Efficiency	Ref.
		Catalyst Loading	Light Source	Exposure Time	Strain	Cell Density		
TiO ₂ P25	anatase-rutile	0.01 mg/mL	Sodium lamp/400W	4 h	<i>S. cerevisiae</i> , <i>C. albicans</i> , <i>A.niger</i>	1 × 10 ⁵ CFU/mL	Completed in 120 min	[114]
TiO ₂ NPs	7 nm	0–10–100 mg	BLB (UV-A)/20W	72 h–14 gg	<i>P. expansum</i>	2.5 × 10 ⁵ conidia/mL	Score = 1.9 vs. 3.2	[115]
TiO ₂ P25	anatase-rutile	n.a.	white light (356 nm)/2 × 15 W	60 min	<i>C. albicans</i>	10 ⁶ CFU/mL	2 log CFU/mL	[123]
TiO ₂ P25	anatase rutile phase	100 mg/L	Natural sunlight	5–6 h	<i>Fusarium</i> sp. spores	10 ² –10 ³ CFU/mL	Completed in 4–5 h	[116]
TiO ₂ /Zn-Al	n.a.	n.a.	UV-A/n.a.	5 days	<i>A. niger</i>	n.a.	Surface coverage (%) = 0–92.6	[121]

^xCFU = colony-forming units; BLB = black light blue lamp; score = visual appearance and scored from 0 to 4 (description in Section 3.3).

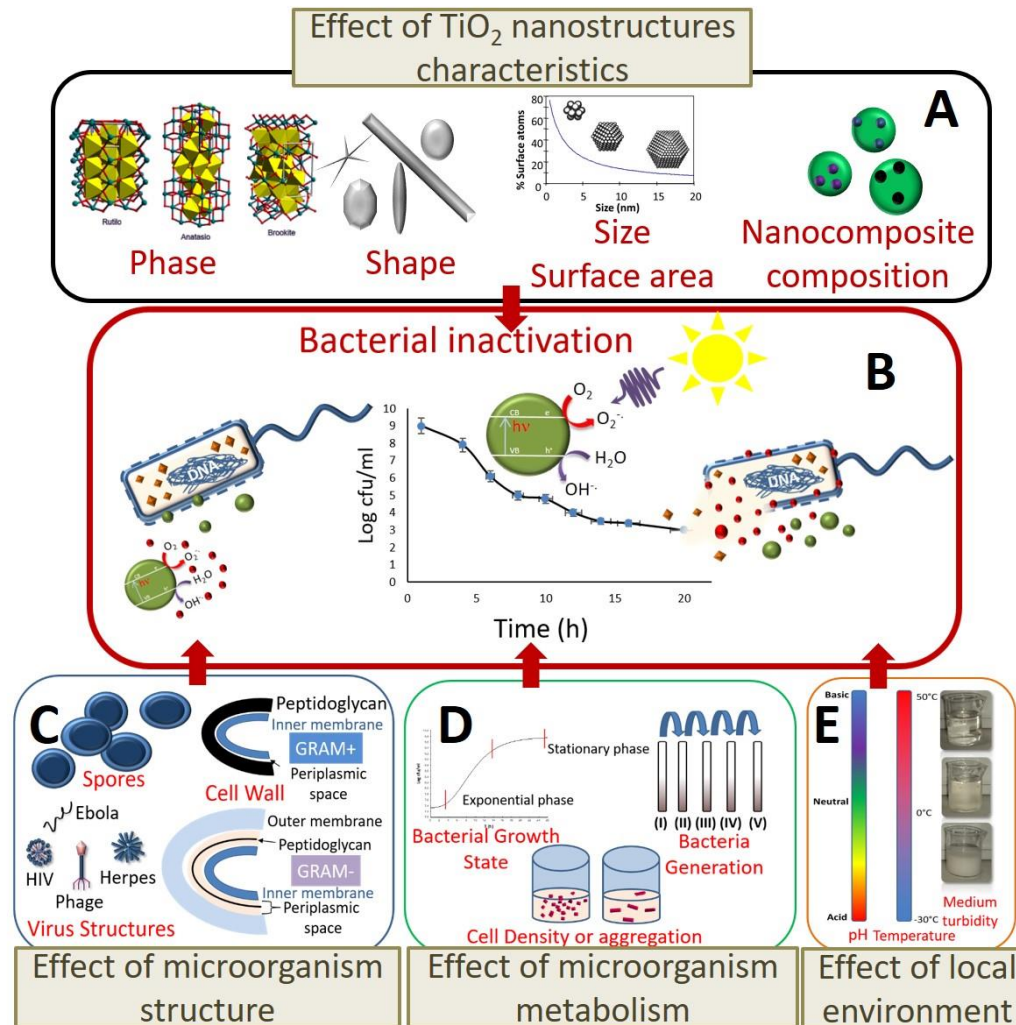


Figure 8. Effect of factors influencing the photocatalytic action of TiO₂ NPs and TiO₂-based nanocomposites on bacterial and viral inactivation: (A) crystalline phase, NP size, and surface area and composition of the nanocomposite affect the photocatalytic efficiency; (C) microorganism structure, (D) its metabolism, and (E) local environment adopted for its growth strongly affect the response of the microorganism to photocatalytic inactivation (B).

Such considerations are intended to point out the relevance of a suitable experimental design, and the need to define reliable and reproducible analytical approaches to studying antimicrobial activity, which could, possibly, also be standardized in order to provide comparable data. In Figure 9, common methods for testing the microorganism inactivation ability of a specific system are outlined.

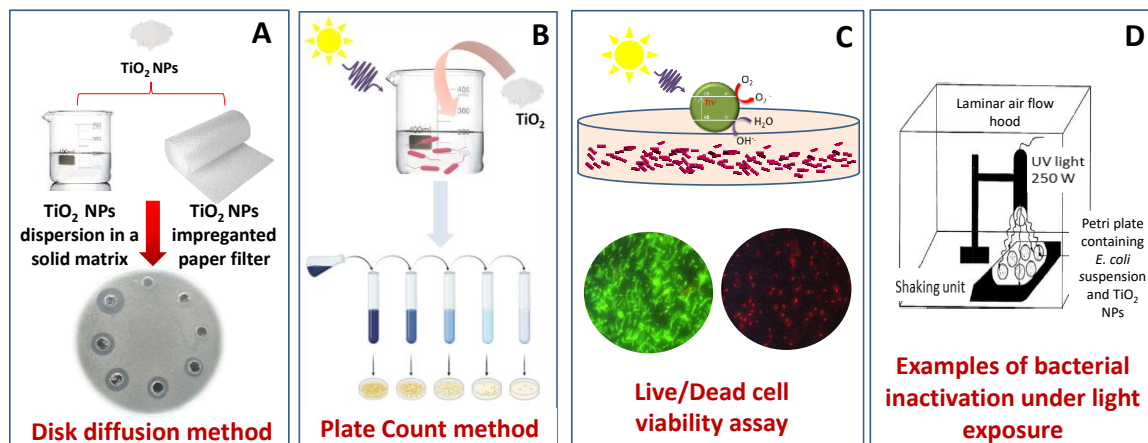


Figure 9. Summary of the reviewed methods to study the antimicrobial activity: (A) disk diffusion method, testing TiO₂ NPs dispersion directly in a solid matrix or impregnated paper filter; (B) plate count of cell suspension in contact with catalyst; (C) live/dead cell viability assay, where the two micrographs show healthy (green) and dead (red) bacteria; (D) examples of experimental set-up by Reddy et al., 2007. Reprinted from ref [82,127], Copyright (2020 and 2016, respectively), with permission from Elsevier.

Antibacterial, antiviral, and antifungal activity on surfaces (fine ceramics) can be evaluated by means of ISO, 27447:2019 (Organization for Standardization) or JIS, R 1702:2012 (Japanese Industrial Standards Committee), ISO 18061:2014 or JIS R1706:2013, and ISO 13125:2013 or JIS R1705:2016 methods, respectively. However, such international standard methods are, in most of the reported cases, not used, or are applied with modification, thus resulting in a large variability in set-up and experimental conditions, that prevent a clear comparison of the performances of the different systems [128–133].

Commonly, antibacterial activity is investigated using the disk diffusion method. According to this approach, NPs are incorporated in a solid matrix or impregnate a paper filter placed on an agar plate (Kirby Bauer agar plating technique). At this stage, bacteria are allowed to grow on the agar plate and the evaluation of the diameter of the inhibitory zones allows to determine the efficiency of bacterial growth inhibition [25,33,134]. In the disk diffusion method, a high number of experimental parameters (different dimensions of spot diameter; cell density used; amount of catalyst) is present, that can, in principle, result in a misled interpretation of the results, thus leading to contradictory conclusions as a function of the different parameters. Although the disk diffusion method is simple and widely used for testing the antibacterial efficiency, it shows some limitations, such as the limited diffusion of the material to be tested in the agar matrix, a poorly resolved concentration gradient around the disks, and the absence of a suitable light source that makes this tool not ideal for the photocatalytic experiments, which require an irradiation source. Therefore, to specifically study the TiO₂-based NPs-assisted photocatalytic inactivation of microorganisms, dedicated experimental set-ups have been proposed, including a proper light source with specifications suitable for the investigation to be carried out [37,61,127,135].

Another issue is caused by the need to evaluate viability or condition of bacteria. For this purpose, a viable count method or the live/dead cell viability assay can be used. The former test allows to simultaneously control the viability of bacteria (live and viable, but not culturable cells), while the latter method allows the simultaneous determination of live and dead cells using two fluorescence dyes: ethidium homodimer III (EthD-III) and calcein acetoxymethyl (calcein AM).

Therefore, the method used to investigate the antimicrobial activity could strongly affect the reliability and interpretation of the experimental results.

Another important issue represented by the need for a standardization of test method is the selection of the microorganism to be used as a target for photocatalytic antimicrobial experiments, especially for a hypothetical future application of the material studied (water-, air-, and food-borne). Beyond the structural properties (i.e., Gram-positive vs. Gram-negative bacteria), the final applications field of the NPs studied should also be considered. Therefore, it is also important to consider the correct indicator microorganism. It follows that the target microorganism can also be selected as a function of the specific application the investigated TiO₂ NPs-based nanocomposite is designed for. In other words, *E. coli*, *Shigella flexneri* (*S. flexneri*), *L. monocytogenes*, and *Vibrio parahaemolyticus* (*V. parahaemolyticus*) are indicators of contaminated waters. They can therefore be selected as target microorganisms for TiO₂ NPs-based nanocomposites specifically designed for water remediation, while indicators of nosocomial infections such as *Streptococcus pyogenes* (*Str. pyogenes*), *Acinetobacter baumannii* (*Acin. baumannii*), *St. aureus*, and *P. aeruginosa* can be used as target microorganisms to investigate TiO₂ NPs-based nanocomposites designed to be used in healthcare facilities.

Taking into account the above reported considerations, it is apparent that the lack of standardized techniques suitable for evaluating the photocatalytic antimicrobial activity of TiO₂ NPs underlining the different actions on the microbial inhibition is at present a strong limitation in unequivocally assessing the photocatalytic antimicrobial properties of TiO₂.

Furthermore, for fungi, the proposed methods to test the antifungal activity may vary significantly in the different reports. Some authors investigate antifungal activity in a fungal suspension containing the TiO₂-based powder irradiating with a light source that can be very different in term of light flux and emission wavelength [82,114,116,117,123]. The photocatalytic activity is evaluated by examining the growth of the investigated fungus by plate count relative to an untreated control sample. As an alternative, the photocatalysts can be applied directly to fruit or vegetable surfaces (e.g., apple, tomato, or lemon) [115,117] and the photocatalytic activity can be evaluated by simply measuring the diameter of the fungal colonies grown with relative to an untreated control sample.

In conclusion, photocatalytically active TiO₂ NPs show great potential for antiviral and antifungal related applications. However, while antiviral activity is well documented, the photocatalysis-promoted antifungal activity of TiO₂ NPs, still deserves more investigation, considering, in particular, the role played by the structural features of the microorganisms in terms of thickness of spores and cell wall.

4. Technological Applications of Antimicrobial TiO₂-Based Nanostructured Materials

In this section, selected applications of the antimicrobial TiO₂-based materials will be described focusing the attention on environmental applications, including water treatment, anti-biofouling membranes for water treatment, disinfection of building materials, and disinfection of (i) biomaterial and (ii) food packaging and processing materials.

4.1. Environmental Applications

4.1.1. TiO₂-Based Nanostructured Materials for Water Disinfection

TiO₂ based nanocomposites are well known and extensively used materials in water treatment technologies [3,4,136]. Indeed they are able, due to their photocatalytic activity, to degrade organic pollutants such as dyes, [137] pesticides [138], pharmaceuticals [3,139], and personal care products [140], that pose a great danger for human and aquatic life. Moreover, their antimicrobial properties are effective against waterborne pathogens such as bacteria, viruses, and fungi that originate from the urban microbiome and tend to be released and accumulated in sewage and urban runoff. The mechanism is summarized in Figure 10 and will be explained in the following. Waterborne diseases derive often from bacteria such as *E. coli*, *Legionella pneumophila*, *Mycobacterium avium*, *S. flexneri*, *L. monocytogenes*, *V. parahaemolyticus* and, to a lesser extent, from viruses, that are typically present at lower concentration.

Every year, waterborne infections cause nearly 200 million deaths worldwide, mainly localized in low income countries [129]. One of the most critical classes of bacteria in wastewater treatment plants (WWTPs) is antibiotic resistant bacteria (ARB), which derive from the extensive use and abuse of antibiotics. WWTPs offer an ideal environment for ARB proliferation and, under these conditions, the antibiotic resistance genes (ARG) that induce the resistance in the bacterial population, can spread easily and quickly. Therefore, as the use of common antibiotics becomes ineffective, it is fundamental to develop alternative strategies to treat microbial infections and to promptly take action against the spreading of ARB in water as well as in the air [141]. The present section will focus on TiO₂-based nanomaterials as an excellent alternative to conventional methods for water disinfection. In addition, nanomaterials applied to counteract the biofouling will be reviewed, as it is another great problem affecting water treatment plants as well as materials in contact with water, including distribution pipes and filtration membranes [142].

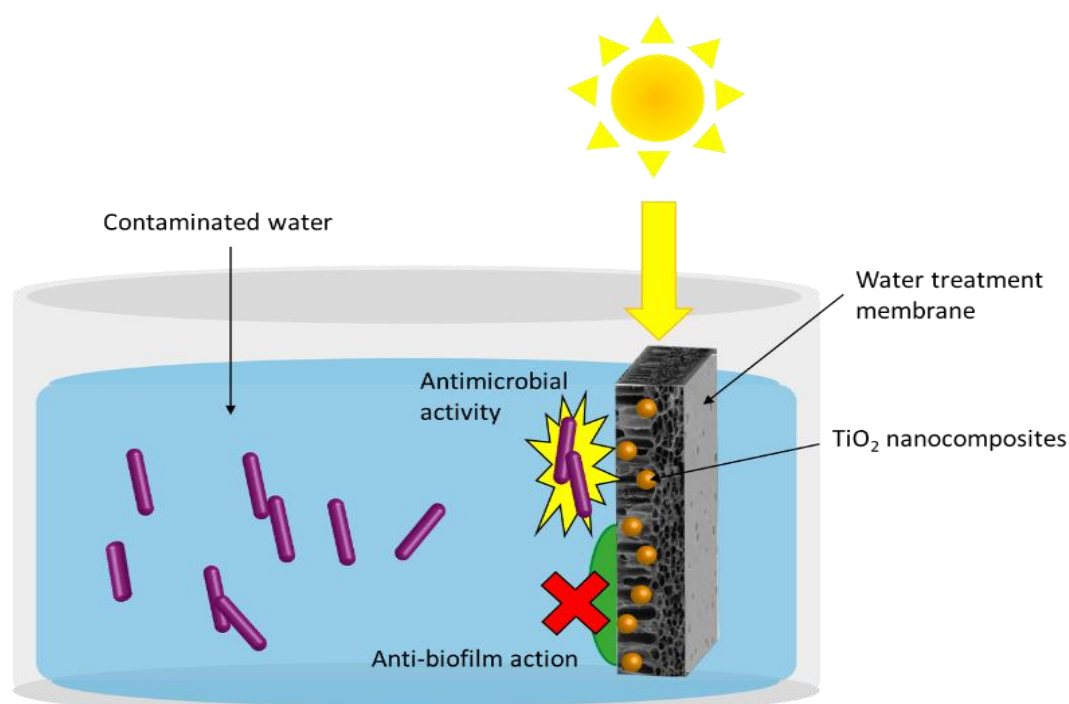


Figure 10. General scheme of TiO₂ NPs-based nanocomposite application for water disinfection, that highlights the ability to prevent biofilm formation at the surface of the substrate, such as a membrane, and the antibacterial activity against water pathogens driven by photocatalysis.

TiO₂ NPs-based nanocomposites for water disinfection are often investigated as colloidal suspensions, since, under these conditions, the whole NPs surface is available, exposing all the active catalytic sites to the aqueous environment dispersing the pathogens. However, while suspended NPs are typically found to display a higher photocatalytic activity in comparison with NPs immobilized on a substrate [143], the dispersed NPs present technological problems, as they need to be recovered to prevent them from becoming a source of pollution in the environment.

Biancullio et al. investigated the effect of TiO₂ NPs on the inactivation of ARBs and antibiotics in urban wastewater and showed that the photocatalytic treatment inactivated *E. coli* and *Enterococci* sp. However, bacteria regrowth experiments demonstrated that the bacteria population over time was not inhibited and that the ratio between resistant and non-resistant cells, detected before and after the TiO₂-assisted photocatalysis treatment, stayed unchanged [144]. Venieri et al. proposed metal-doped TiO₂ (Mn-, Co-, and binary Mn/Co-doping) nanomaterial against *K. pneumoniae* in real wastewater. After 90 min of exposure to artificial sunlight, a decrease in bacterial population, in the range from 4 to 6 logs cycles, was measured in each investigated case and the co-doped material (0.04% wt)

was found to be effective like the single doped (0.1% wt) samples. Nevertheless, the experiment performed under natural sunlight irradiation showed a lower photocatalytic efficiency, as a 2-log bacteria population reduction was detected in presence of the Mn/Co-TiO₂ nanocomposite. Moreover, the resistance of the bacteria surviving cells to some antibiotics was found to be decreased even though ARGs were still detectable, and thus found to be potentially able to develop antibiotic resistance [39]. Rizzo et al. reported the antibacterial activity of N-doped TiO₂ NPs against the antibiotic resistant *E. coli* from urban wastewater. They found a higher activity of N-doped TiO₂ NPs compared to the commercial benchmark TiO₂ P25 and identified 0.2 g/L NPs concentration suited to obtain, under simulated sunlight irradiation, the highest inactivation rate (8.5×10^5 CFU 100 mL⁻¹min⁻¹) after 10 min of irradiation and total inactivation after 60 min. No significant change in *E. coli* resistance to selected antibiotics (ciprofloxacin, cefuroxime, tetracycline, and vancomycin) was observed after treatment [145]. The same authors investigated the effect of TiO₂ P25 on the same bacteria as a function of irradiation type, testing four different light sources: a wide spectrum 250 W lamp, the same lamp equipped with a filter to simulate solar radiation, a 125 W black light fluorescent lamp, and real solar light. A higher efficiency was found when artificial solar light was used to irradiate for 60 min 0.05 g/L of TiO₂ suspension with respect to solar light. Differences in antibiotic resistance were detected as a function of the irradiation source. On the other hand, the unfiltered 250 W lamp was able to inactivate *E. coli* without any catalysts, whereas the 125W black light fluorescent lamp catalyzed a 70% inactivation of *E. coli* in the presence of 0.1 g/L of TiO₂ [146].

Ghosh et al. described an antibacterial activity, under UV-vis irradiation of a Ag-TiO₂ nanocomposite, obtained upon ball-milling of Ag and P25, against *E. coli* and *St. aureus* higher than that of the bare TiO₂ NPs. A similarly high photocatalytic efficiency was observed for the degradation of organic molecules. The nanocomposite was found not to be cytotoxic below a 50 µg/mL concentration [49]. Liu et al. proposed a vertical face-to-face heterojunction obtained by assembling horizontally TiO₂ nanosheets, exposing 001 facet, with graphitic carbon nitride (g-C₃N₄) sheets, obtaining a Z-scheme electron transfer that enhances the charge separation and therefore the photocatalytic and antibacterial activity. In particular, a 96.8% reduction of *E. coli* was achieved after 30 min of simulated solar light irradiation, against a 50% reduction obtained with unmodified TiO₂. In the dark, the nanocomposite promoted only a 5% reduction of the *E. coli* population after 30 min, thus confirming that the bacteria inactivation occurred mainly due to photocatalytic ROS production [45]. Liga et al. evaluated the biocide activity, both at dark and under UV-A irradiation, of Ag-TiO₂ obtained by photoreduction of AgNO₃, against bacteriophage MS2, a model virus for common waterborne pathogens, characterized by a high resistance to common water disinfection methods. The inactivation activity of this system under UV was up to five times higher than that observed for commercial TiO₂ P25 and was found to enhance with the increase of the Ag amount [49].

Kim et al. reported on a nanocomposite based on TiO₂ NPs coupled with glucose oxidase (GOx), an enzyme acting as organic biocatalyst in presence of glucose, purposely selected as a high concentration of glucose favours the proliferation of heterotrophic bacteria, thus providing a (photo)catalytic system able to decrease the amount of available glucose and, concomitantly, to increase the production of reactive species, responsible for bacteria inactivation. Under UV irradiation with a 4W UV lamp ($\lambda_{\max} = 352$ nm), inactivation of *E. coli* assisted by TiO₂-GOx was higher than that assisted by bare TiO₂, and such enhancement was much more relevant in the presence of glucose [52].

4.1.2. Immobilization of Nanocomposites on Membranes or Recoverable Supports

The immobilization of photocatalytic TiO₂ NPs and their nanocomposites onto a suitable substrate is essential to accomplish technologically feasible applications. As mentioned above, a robust and durable immobilization of NPs onto appropriate support is fundamental, not only for enabling the nanosized photocatalyst recovery, but also to prevent the accidental release of NPs in the environment, that, becoming themselves a possible contaminant, may become harmful [4]. Here, some of the most

original proposed solutions for the deposition and immobilization of TiO₂ NPs-based nanomaterials specifically designed for photocatalytic microorganism inactivation are summarized.

Li et al. developed a foam based on photocatalytic TiO₂ NPs; a promptly separable system, and, as it floats at water surface, it is able to efficiently exploit sunlight for photocatalytic generation of ROS [147]. Another ingenious solution is based on nanocomposites also incorporating a magnetic domain, able to convey to the system magnetic properties effective in enabling their simple recovery at the end of the treatment by applying a magnetic field. Wu et al. synthesized a ternary composite based on lanthanum-doped TiO₂/calcium ferrite/diatomite with magnetic properties, and enhanced photocatalytic antibacterial activity against *E. coli* [46]. Another interesting alternative to achieve recoverable photoactive materials is given by nanocomposites formed of NPs coupled with micrometer structures, thus combining the advantages of the nanoscale properties with the possibility of recovering the composite by using filtration methods. Indeed, Xiao et al. reported an original multifunctional system, based on chitosan (CS) beads decorated with TiO₂ nanostructures modified with Ag NPs, able to effectively merge the advantage of a recoverable and reusable material and an enhanced antibacterial activity, synergistically accomplished by each of the three components of the nanocomposite, as effectively demonstrated against *E. coli* upon UV-A irradiation [50].

Negishi et al. used a similar approach with commercial TiO₂ coated silica gel beads (4 mm diameter). The coated beads were applied in a solar water purification system for disinfection of tap water from a village in Thailand. A reduction of coliform and general bacteria was observed during three days, together with a degradation, after long time exposure, of the silica component of the bead, resulting in loss of the TiO₂ layer. [148]

However, the most extensively explored immobilization approach relies on the incorporation of the photocatalyst in polymeric materials [149]. In particular, polymeric membranes have been thoroughly applied in water treatment technologies as microfiltration, ultrafiltration, nanofiltration, membrane bioreactors, and membrane with biocide activity for water disinfection, through the integration of TiO₂ nanostructured material [150]. Haghghat et al. designed a nanocomposite Ag/TiO₂/polyvinyl chloride (PVC) membrane for ultrafiltration (UF) by incorporating well dispersed Ag/TiO₂ NPs in the host polymer. Such a nanocomposite-based membrane displayed bacterial inactivation ability against *P. aeruginosa*, *E. coli*, and *St. aureus*, together with antifouling properties and degradation activity against an organic dye [51]. Li et al. reported a nanofiltration (NF) membrane obtained by coating a polyethersulfone (PES) substrate with a film of nanocomposite consisting of TiO₂ NPs (functionalized with tannic acid) embedded in polyester. In particular, the membrane prepared with 0.020 wt% TiO₂ tannic acid (TA) solution showed an *E. coli* population reduction of 77.2% under dark conditions and a 99.2% *E. coli* population reduction after UV irradiation at 365 nm [54].

Photocatalytic membrane reactors (PMRs) combine the membrane technology with the advantages of photocatalysis assisted reactions. Two main configurations are reported in the literature: PMRs with the photocatalyst immobilized on the membrane or incorporated therein, and PMRs based on the photocatalyst dispersed in a colloidal suspension. In both cases the photocatalyst is confined in the reaction environment. However, the former configuration allows an effective recovery and reuse of the catalyst, thanks to its stable immobilization, while the recovery is more complicated in the latter case, although the whole NPs surface can be more effectively exploited for adsorption and catalysis [151]. Among the possible photocatalysts for PMR fabrication, TiO₂ NPs and TiO₂ NPs-based nanocomposites have been the most investigated [152]. Cheng et al. fabricated a PMR based on the combination of a polyvinylidene fluoride (PVDF) membrane and a suspension of TiO₂ P25 in tap water and studied the biocide effect for virus removal, using phage *f2* as a model. The effect of the amount of humic acid (HA) in the water dispersion on the efficiency of the system was also investigated. Moreover, HA was found to compete with phage *f2* at the adsorption sites on TiO₂ NPs surface, and the UV light absorbed by HA overall led to a reduction of biocide activity at high HA concentration [153]. A PMR based on a microfiltration hollow polyethylene (PE) fiber membrane coupled with a suspension of TiO₂ P25 was investigated for the reduction in bacterial population of secondary effluent water

sample, that was assessed, down to 2 log, when a 1g/L TiO₂ NPs suspension was used [154]. Another typical and efficient approach for nanocatalyst immobilization, able to preserve their activity, relies on their immobilization onto fibers that, possessing a high surface, allow optimal interaction between the target substrate dispersed in water and the photocatalyst. Amarjargal et al. functionalized the surface of electrospun polyurethane (PU) fibers with Ag-TiO₂ NPs by simply dipping the fiber in hot colloidal photocatalyst dispersion for 4 h and 12 h. After 3 h UV irradiation (320–500nm), a 6-log cycles reduction of *E. coli* population was found for the sample obtained after 4 h immersion and a 5-log cycles reduction for that immersed for 12 h. Interestingly, only 2-log cycles reduction was detected after exposure to UV, in absence of Ag-TiO₂ and no reduction was observed upon exposure of the nanocomposite to ambient light [35]. The antibacterial activity of electrospun Ag-TiO₂ nanofibers was tested against *E. coli*. The study demonstrated that, under the investigated experimental conditions: (i) no biocidal activity was obtained upon exposure to light (solar simulator) of the bare fiber, nor in the dark for TiO₂/Ag fibers and P25-coated fibers, (ii) fibers functionalized with the synthesized TiO₂ performed better, in terms of photocatalytic antibacterial activity, than fibers coated with TiO₂ P25, and (iii) the antibacterial activity in presence of Ag NPs was found higher in the dark than under light irradiation [155]. A TiO₂/Polyamide 6 (PA-6) electrospun fiber was tested by Daels et al. for the removal of *St. aureus* and HA from a secondary effluent sample. HA reduction of 83% after 2 h irradiation with simulated solar light (300 W Osram Ultra-Vitalux lamp) with an intensity of about 5 mW/cm² and 99.99% bacteria reduction after 6h UV irradiation was detected. The same fibers, tested in a filtration process (flow rate 11 m³/(m²h)) in a photocatalytic experiment performed under UV irradiation achieved 37% HA reduction and 76% *St. aureus* inactivation [18]. Zheng et al. electrospun Cu-TiO₂ nanofibers and tested the biocide activity under visible light against *f2* phage and the system formed by *f2* phage and *E. coli* as its host, and reported a photocatalytic inactivation of *E. coli* higher than that of *f2* phage. Remarkably, the *E. coli* inactivation did not seem affected by the presence of *f2* phage, while the inactivation of the phage *f2* in the bacteria host system was lower than that found in absence of *E. coli*. Such a result was explained by considering that *E. coli* can behave as a ROS scavenger, probably due to its membrane structure, as discussed above, thus reducing amount of ROS effective for *f2* inactivation, thus somehow preventing its inactivation [108].

Ishikawa et al. proposed an interesting approach to obtain ceramic fibers characterized by an outer TiO₂ NPs enriched layer. Namely polycarbosilane, -SiH(CH₃)-CH₂-)_n, was mixed with Ti(OC₄H₉)₄ (50 wt%) in order to obtain a fiber by melt spinning, that was then exposed to air at 70 °C for 100 h. The resulting fiber was composed of amorphous SiO₂ and nanometric TiO₂ in anatase phase that, for a bleed-out process, migrated to the surface of the fiber. The functionalized fiber demonstrated an ability to completely remove coliform from wastewater after 3 h UV irradiation (352 nm, 2 mW/cm²) [156].

4.1.3. Anti-Biofouling Membranes for Water Treatment

The biofouling process is defined as the accumulation of microorganisms on a surface, and is realized in four steps: (i) organic matters are adsorbed on the surface, (ii) microorganisms adsorb and adhere to the surface, and (iii) start to grow and reproduce on the surface, and finally (iv) extracellular polymers are secreted and mutual adhesion among the clonal cells takes place [157]. These processes ultimately result in the formation of a biofilm, namely an assembly of microbial cells, irreversibly bound to a surface and embedded in a matrix of polysaccharide material [158]. When biofouling takes place at the surface of a membrane, its flux is limited, thus interfering with rejection and reducing the lifetime of the membrane itself, with the consequent drawbacks. In order to prevent biofilm formation, two main strategies can be employed. The first relies on the ability to enhance the hydrophilicity of the membrane, which reduces the affinity of the organic matter, and enhances its affinity with water, that can, thus, form a thin layer on the membrane surface, finally hampering the microorganisms' adhesion. The second route is based on the incorporation of antibacterial agents into the membrane, such as TiO₂-based nanomaterials [51]. TiO₂-based nanocomposites are greatly suggested for this application since they display antibacterial properties and, concomitantly, convey, as a function of

their chemical nature, hydrophilicity to the host membrane [159]. The combination of the intrinsic antibacterial properties with the photocatalytic properties of TiO₂ NPs-based nanocomposites offers multiple advantages for hindering the biofouling. As an example, Kim et al. deposited TiO₂ NPs on a polyamide thin film composite (TFC) membrane and tested their anti-biofouling properties, along with the antibacterial activity against *E. coli*. The water flux was measured for three days, for pristine and TiO₂ NPs-modified membrane, and with and without UV-light irradiation. After pipetting *E. coli* dispersion onto the membranes and incubating at 37 °C, a fast and significant reduction of the flux, a clear indication of the occurrence of a higher fouling, was observed for the membranes not exposed to UV, while a slow and low reduction of the flux was found for TiO₂-modified membranes, especially upon UV irradiation, finally demonstrating how the anti-biofouling activity is tightly connected to antibacterial behavior of UV-active TiO₂ photocatalysts [19].

4.2. TiO₂ NPs-Based Nanocomposite against Biofouling on Building Materials

In the construction field, nanostructured TiO₂ is commonly employed to degrade organic pollutants in the air or to protect the building materials from soot, due to its photocatalytic and hydrophobic properties. The biocide activity of TiO₂ can also be exploited to reduce the formation of biofilms formed on the surface of buildings [160]. Indeed, biofouling causes, not only aesthetic and structural degradation of construction materials and surfaces, but also bacteria and fungi proliferation that may pose a great health concern [149]. The application of photocatalytic TiO₂ NPs as a biocidal agent has considerable relevance, especially for locations strongly sensitive to biological safety, such as medical facilities and food industries, where usually ceramic tiles are used to coat walls and floor. The photocatalytic activity of TiO₂ nanomaterials was found to successfully reduce the bacterial proliferation and the fungi population (and, consequently, mycotoxins production) indoor when applied to surfaces, tiles, furniture etc. [161]. Dyshlyuk et al. tested suspensions of TiO₂, ZnO, and SiO₂ against microorganisms known for damaging construction materials, namely a bacterium (*B. subtilis*) and several common fungi (*A. niger*, *Aspergillus terreus*, *Aureobasidium pullulans* var. *pullulans*, *Cladosporium cladosporioides*, *Penicillium ochrochloron*, *Trichoderma viride*, and *Paecilomyces variotii*). They found TiO₂ and SiO₂ less active under sunlight than ZnO [162]. Sikora et al. fabricated core-shell nanocomposites of mesoporous silica (mSiO₂, core) and TiO₂ (shell) to be applied on cement mortars. The merging of the two nanomaterials in one nanocomposite was found to play the two roles of introducing in the building material a filler, mSiO₂, able to improve its mechanical properties, and conveying, with TiO₂, anti-biofouling and self-cleaning activity upon UV exposure. The mSiO₂/TiO₂ composite antibacterial activity was tested against *E. coli* and, after 2 h, a 67% and a 42% reduction were measured after exposure to UV light and at dark, respectively [46].

4.3. Photocatalytic TiO₂ NPs-Based Nanocomposites for Biomaterials Disinfection

Antibacterial NPs find a wide range of applications in the field of biomaterials. Materials designed for wound dressing or for tissue engineering-related applications need to comply with several requirements as summarized in Figure 11, as they need to be biocompatible, non-allergenic, easily removable, and degradable after implantation.

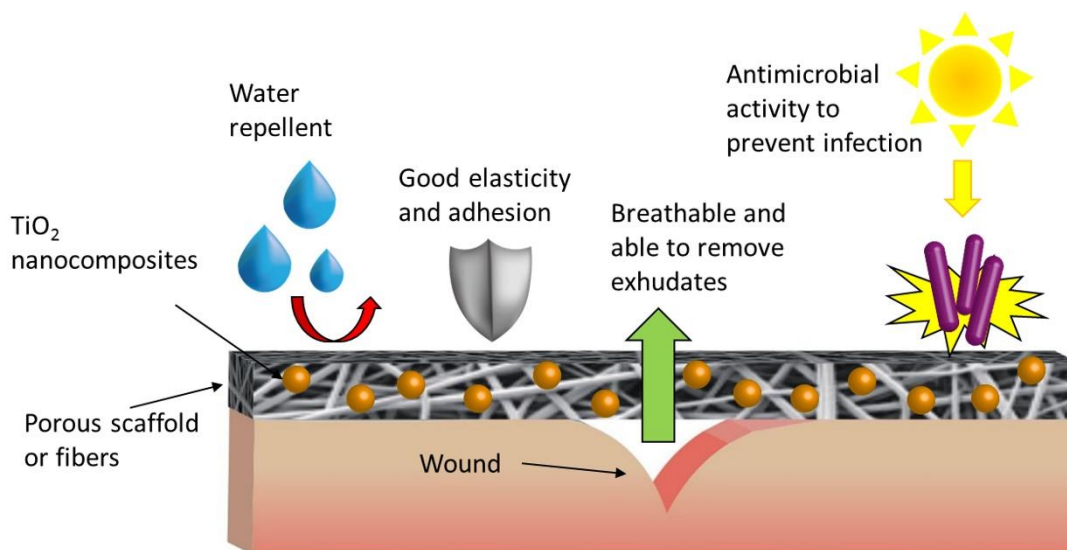


Figure 11. General scheme of TiO_2 NPs-based nanocomposite application for biomaterial-related applications highlighting the ability to repel water, to adhere to the skin following its movements, to remove exudates, to be permeable to air, and to prevent infections due to the antimicrobial activity driven by photocatalysis.

Antibacterial behavior is strongly desirable in this kind of material to prevent infections during wound recovery [163,164]. A great deal of work has been carried out in the development of biocompatible TiO_2 -NPs-based nanocomposites, with intrinsic antimicrobial activity, specifically designed for tissue engineering-related applications to be used in healthcare facilities [33,165–169].

In this scenario, several research groups have explored the advantages of TiO_2 -based nanocomposites considering both their biocompatibility and the intrinsic antibacterial properties, focusing also on their excellent photocatalytic properties that can be extremely advantageous in specific biomedical applications. Monmaturapoj et al. fabricated a nanocomposite made of TiO_2 and HAP NPs for face masks serving as filtration devices. HAP is a type of calcium phosphate-based ceramic material widely used in the biomaterial field, especially in orthopaedic implants, being biocompatible and a very good substitute for bone. After assessing the antibacterial activity of the nanocomposite, [170] strong antiviral activity against H1N1 influenza A virus was observed under UV-light irradiation, with a synergic effect of HA and TiO_2 NPs that revealed optimal for HA/ TiO_2 (50:50) [53]. Li et al. coated a face mask for medical purposes with NPs formed of a mixture of silver nitrate and TiO_2 NPs in order to work as photocatalyst, reduce the bacteria population and to inhibit their growth on the surface, due to the presence of the exhaled moisture from breathing. A 100% reduction of bacteria on the surface of the coated mask 24 h after *E. coli* and *St. aureus* inoculation was found against a 25% and 50% increase measured on the uncoated masks for the two bacteria, respectively [171].

4.4. TiO_2 NPs-Based Nanocomposites Designed for Disinfection of Food Packaging and Processing Materials

Food packaging materials containing TiO_2 NPs-based nanocomposites have been thoroughly investigated materials for food contact-related applications and a steadily increasing number of technologies has been in development in the last years. This is in order to accomplish multiple purposes including improved mechanical, thermal, optical and antimicrobial properties, control of gas and moisture permeability, UV shielding, nutraceuticals release, and installing sensors for pathogens and harmful substances (Figure 12) [172–174]. Indeed, surfaces of food-processing plant components need to comply with the same requirements, as they are often in contact with food and the presence of microorganisms therein can easily lead to food contamination, causing transmission of diseases [153]. Indeed, the presence of antimicrobial substances in food packaging materials may inhibit growth of harmful microorganisms and pathogens on food, improving its safety and shelf

life. NPs and nanocomposites can be integrated in food packaging materials as growth inhibitors, antimicrobial agents, or carriers [175], and are usually applied to the packaging of meat, fish, poultry, bread, cheese, fruits, and vegetables [176]. TiO₂ NPs, aside from antibacterial properties, also possess unique characteristics that may prove particularly useful for such applications. For example, TiO₂ shields UV light, a property that is generally exploited in the formulation of sunscreen lotions, and therefore may be an effective additive in packaging to preserve food from irradiation, and thus limit its deterioration [177,178]. Moreover, when TiO₂ NPs are contained in a packaging material, upon UV exposure they can photocatalytically degrade the ethylene molecules produced during the ripening process, which are responsible for food degradation [179].

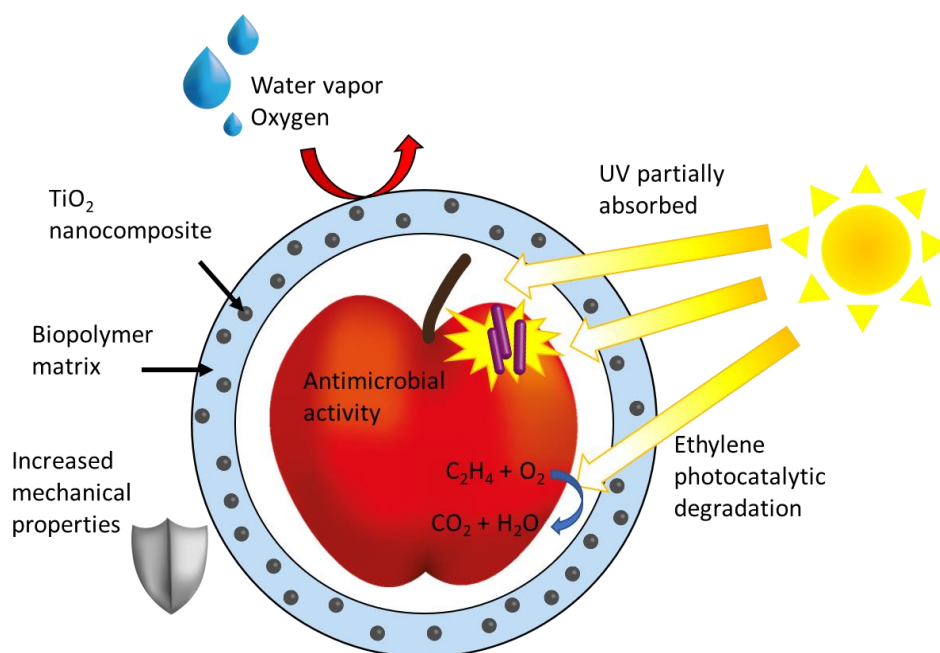


Figure 12. General scheme of TiO₂ NPs-based nanocomposite application for food packaging highlighting the advantages of TiO₂ in the coating as improved mechanical properties, water and oxygen repellence, UV shielding, and ethylene scavenger and antimicrobial activity.

In the last years, the choice of a polymer suitable and environmentally sustainable for food packaging has oriented towards biopolymers, which can be easily degraded and recycled, for a more ecological fingerprint in a field that has been, so far, heavily relying on petroleum-based polymers. Such biopolymers include poly hydroxybutyrates (PHB), polylactic acid (PLA), poly caprolactone (PCL), polyvinyl alcohol (PVA), poly butylene succinate, lipids (wax and free fatty acids), proteins (casein, whey, and gluten), polysaccharides (starch and cellulose derivatives, alginates, and chitosan) and their possible blends [180]. In particular, chitosan, a polysaccharide derived from chitin, is especially suited for food packaging, considering, as reported above, its biocompatibility, biodegradability, and antibacterial and antifungal behavior, along with good film forming properties [177,181].

Zhang et al. developed a coating for food packaging based on TiO₂ NPs embedded in a chitosan (CS) matrix. The presence of TiO₂ NPs in a chitosan film served to improve, upon exposure to visible light, its mechanical properties, wettability and antibacterial activity against typical food pathogens (*E. coli*, *St. aureus*, *C. albicans*, and *A. niger*) with respect to film formed by bare chitosan. The effect of the direct application of the CS/TiO₂ coating on red grapes was also tested and was shown to preserve the fruit better than conventional plastic coating [181]. Li et al. reported a composite film where Ag-TiO₂ nanocomposites were embedded in a mixture of fish gelatin (FG) and CS, given that FG is a protein with good film forming, and antioxidant and water locking properties. The addition of CS imparted to FG enhanced mechanical properties while the integration of the Ag-TiO₂ nanocomposite, to a different

extent, conveyed antibacterial activity. Antibacterial activity (against *E. coli*, *St. aureus*, and *Botrytis cinerea*) and UV-blocking function were found to increase as a function of Ag-TiO₂ concentration. However, its very high content led to a deterioration of the mechanical properties of the composite, that were observed, which instead, improved at low Ag-TiO₂ concentration [182]. Xu et al. realized a coating based on three different antimicrobial agents: graphene oxide (GO), chitosan and TiO₂ NPs, in increasing amounts. The sample with intermediate TiO₂ NPs concentration (GO:CS:TiO₂ ratio of 1:20:4) showed a good antimicrobial activity against *B. subtilis* and *A. niger*, and proved able to destroy bacterial cell membrane and to avoid the formation of a biofilm. Such a coating, when applied to fruit and vegetables, such as strawberries and mango, was found suitable to delay weight loss, which is caused by deterioration, to reduce polyphenol oxidase (PPO)—the enzyme responsible for food browning—activity, and to increase superoxide dismutase (SOD) activity, which is usually high in low stress conditions for the fruit. [47]

Besides chitosan-based blends, many other polymers have been used recently to develop antimicrobial composite coatings containing TiO₂ NPs for food packaging. Xie et al., for example, embedded TiO₂ NPs into three different biodegradable polymers: cellulose acetate (CA), polycaprolactone (PCL), and PLA. A higher compatibility of TiO₂ with CA and PLA was observed, along with improved film forming properties, resulting in uniform films. Moreover, the CA/TiO₂-based films showed a high transparency, and good photocatalytic activity, as demonstrated by degradation of methylene blue upon irradiation with a UV-A light. The best antibacterial activity under the investigated experimental conditions, when compared to the other systems, was found against *E. coli* upon 2 h UV-A light irradiation with light intensity of 1.30 ± 0.15 mW/cm², and was found to increase at higher TiO₂ concentration, achieving a 1.69 log CFU/mL reduction. Very low reduction was, instead, observed, even at the highest TiO₂ concentration, without irradiation [183]. Xie et al. thoroughly investigated the behavior of the best performing CA/TiO₂ coatings when the bacteria were inoculated under the coating itself and—upon UV-A exposure—a higher TiO₂ concentration was found to act as a screen, decreasing the intensity of the light reaching the inoculum and resulting in reduced antibacterial activity [184].

He et al. realized a uniform coating using fish skin gelatin and TiO₂ in different ratios (30:1, 20:1, 10:1). The film showed antibacterial activity increased when TiO₂ was embedded, reaching values of 54.38% and 44.89% for *E. coli* and *St. aureus*, respectively, for the sample with the highest TiO₂ content (10:1 ratio) after 2 h UV irradiation. Moreover, the presence of TiO₂ enhanced tensile strength and elongation at break and reduced water vapor permeability of the coating. The coating, transparent in the visible region, was found to act as a barrier against UV-C light [175]. Teymoupour et al. reported a composite coating based on a soluble soybean polysaccharide (SSPS) as biopolymer. The SSPS/TiO₂ coating, obtained at increasing TiO₂ concentration—0%, 1%, 3%, and 5% (*w/w*)—resulted in an increased antibacterial activity against both *E. coli* and *St. aureus*, being particularly effective against *St. aureus*. Properties such as water vapor permeability, oxygen permeability, and moisture content decreased upon the addition of TiO₂, while the mechanical properties improved [185].

All the application of any kind of NPs in materials that come into contact with food must cope with NP migration and their release, as it may become a severe environmental hazard [177,178]. Although in the last decade many strategies have been proposed to improve quality standard for food-contact materials and to reduce its impact on the environment, the regulations concerning nanocomposite based coatings for food safety remain behind, thus further delaying their development up to market [179].

5. Conclusions and Perspectives

Pathogenic microorganisms have demonstrated the ability to spread easily throughout the world, thus potentially very severely threatening human health, as the current COVID-19 pandemic has shown in the last year. Therefore, inactivation of pathogenic microorganisms in water, on surfaces, and on food strongly demands the attention of the scientific community. Photocatalytic TiO₂-based nanomaterials have demonstrated their potential to tackle pathogens through multiple paths, in

particular by exploiting light (even sun or ambient light, in some cases) to photocatalytically generate ROSs able to kill them or inhibit their growth without using chemical products, that may, instead, be even more harmful for human health and the environment. However, to realistically make the great promise of these photocatalytic nanomaterials viable, it is necessary to easily access large amounts of TiO₂-based nanomaterials with controlled size, crystalline phase, and surface chemistry. Such a consideration has been, therefore, briefly summarized in the first part of the review, reporting examples of promising synthetic approaches, specifically selected for their potential scalability towards TiO₂-based nanomaterial production, thus ultimately showing the great contribution of modern materials science in providing an extremely rich toolbox for manufacturing nanomaterials with designed photocatalytic properties.

In the second part of the review, we critically analyzed selected approaches within the plethora of reported ones to investigate the antimicrobial properties of TiO₂-based nanomaterials. While all the described examples have shown the capability of TiO₂-based nanomaterials in inactivating bacteria, fungi, and viruses, the great variability of the experimental parameters (catalyst loading, light source and intensity, target microorganism, environmental conditions of microorganism growth, method of detection of antimicrobial efficacy) used in the antimicrobial tests does not allow an objective comparison of the reported results nor to trace a profile of antimicrobial activity efficiency across the different proposed and investigated TiO₂-based nanostructured materials. In addition, the selection of the target microorganism needs to be carefully designed as a function of the intended application. Moreover, a more fundamental issue that makes it very complex to correctly interpret the outcome of experiments is given by the multiple mechanisms of TiO₂ NPs antimicrobial activity concomitantly occurring, that, as reported, could involve an intrinsic antimicrobial effect of TiO₂-based nanomaterials in the dark. It follows a strong need for standardized protocols and methods specifically suited to quantitatively evaluate the photocatalytic antimicrobial activity of TiO₂ NPs, and thus compare the performance of the materials. In this way, it would be possible to highlight the role of the different inhibition mechanisms of the investigated materials, under the specific conditions.

Finally, established and standardized characterization tools to elucidate photocatalytic antimicrobial activities would also fully empower a sound investigation of a systematic structure-function relationship that could be applied not only to TiO₂-based nanomaterials but also to whole classes of photocatalytic nanomaterials.

Nonetheless, the results reported so far are promising, as can be inferred by the maturity level of the technological applications that, in a few cases, have been already obtained, as discussed in the third part of the review. Indeed, photocatalytic TiO₂-based nanomaterials have been recently successfully exploited in the disinfection of urban wastewater, in the production of photocatalytic anti-fouling membrane for ultra- and nanofiltration, to prevent building materials from bio-fouling, for biomaterials disinfection in wound dressing application and mask filters, and for the disinfection of food packaging and processing materials.

In conclusion, photocatalytic TiO₂-based nanomaterials hold great promise in the fight against a wide range of pathogenic microorganisms that can be effectively inactivated and destroyed in different matrices, including water, air, surfaces, and food, possibly also providing additional weapons against extremely harmful and emerging strains like the SARS-CoV viruses.

Author Contributions: I.D.P., R.C. and M.L.C. conceived and drafted the work. I.D.P., F.P., C.L.P. and M.D. designed the article, and acquired, analyzed, and interpreted the literature reports. A.A. critically revised the manuscript. All authors have read and agreed to the published version of the manuscript.

Funding: This work was partially supported by the Apulia Region Funded Project FONTANAPULIA (WOBV6K5) Italy and the European H2020 funded Project InnovaConcrete (G.A. n. 760858), PON Energy for TARANTO (ARS01_00637). PON Ricerca e Innovazione 2014–2020 (DOT1302393).

Conflicts of Interest: The authors declare no conflict of interest. The funders had no role in the design of the study; in the collection, analyses, or interpretation of data; in the writing of the manuscript, or in the decision to publish the results.

References

1. Laxma Reddy, P.V.; Kavitha, B.; Kumar Reddy, P.A.; Kim, K.-H. TiO₂-based photocatalytic disinfection of microbes in aqueous media: A review. *Environ. Res.* **2017**, *154*, 296–303. [[CrossRef](#)]
2. Li, Q.; Mahendra, S.; Lyon, D.Y.; Brunet, L.; Liga, M.V.; Li, D.; Alvarez, P.J.J. Antimicrobial nanomaterials for water disinfection and microbial control: Potential applications and implications. *Water Res.* **2008**, *42*, 4591–4602. [[CrossRef](#)]
3. Petronella, F.; Truppi, A.; Sibillano, T.; Giannini, C.; Striccoli, M.; Comparelli, R.; Curri, M.L. Multifunctional TiO₂/Fe_xO_y/Ag based nanocrystalline heterostructures for photocatalytic degradation of a recalcitrant pollutant. *Catal. Today* **2017**, *284*, 100–106. [[CrossRef](#)]
4. Petronella, F.; Truppi, A.; Ingrosso, C.; Placido, T.; Striccoli, M.; Curri, M.L.; Agostiano, A.; Comparelli, R. Nanocomposite materials for photocatalytic degradation of pollutants. *Catal. Today* **2017**, *281*, 85–100. [[CrossRef](#)]
5. Khezerlou, A.; Alizadeh-Sani, M.; Azizi-Lalabadi, M.; Ehsani, A. Nanoparticles and their antimicrobial properties against pathogens including bacteria, fungi, parasites and viruses. *Microb. Pathog.* **2018**, *123*, 505–526. [[CrossRef](#)]
6. Lusvardi, G.; Barani, C.; Giubertoni, F.; Paganelli, G. Synthesis and Characterization of TiO₂ Nanoparticles for the Reduction of Water Pollutants. *Materials* **2017**, *10*, 1208. [[CrossRef](#)] [[PubMed](#)]
7. Qarni, F.; Alomair, N.; Mohamed, H. Environment-Friendly Nanoporous Titanium Dioxide with Enhanced Photocatalytic Activity. *Catalysts* **2019**, *9*, 799. [[CrossRef](#)]
8. Petronella, F.; Truppi, A.; Dell'Edera, M.; Agostiano, A.; Curri, M.L.; Comparelli, R. Scalable Synthesis of Mesoporous TiO₂ for Environmental Photocatalytic Applications. *Materials* **2019**, *12*, 1853. [[CrossRef](#)] [[PubMed](#)]
9. Meng, S.H.; Jun, Y.; Li, H.G.; Du, S.G. Using a Sol-Gel Method to Prepare the TiO₂/CNTs Nanocomposite. *Appl. Mech. Mater.* **2014**, *529*, 108–111. [[CrossRef](#)]
10. Meng, A.; Zhang, L.; Cheng, B.; Yu, J. Dual Cocatalysts in TiO₂ Photocatalysis. *Adv. Mater.* **2019**, *31*, 1807660. [[CrossRef](#)]
11. Kang, X.; Liu, S.; Dai, Z.; He, Y.; Song, X.; Tan, Z. Titanium Dioxide: From Engineering to Applications. *Catalysts* **2019**, *9*, 191. [[CrossRef](#)]
12. Cassaignon, S.; Koelsch, M.; Jolivet, J.-P. From TiCl₃ to TiO₂ nanoparticles (anatase, brookite and rutile): Thermohydrolysis and oxidation in aqueous medium. *J. Phys. Chem. Solids* **2007**, *68*, 695–700. [[CrossRef](#)]
13. Lee, D.S.; Liu, T.K. Preparation of TiO₂ Sol Using TiCl₄ as a Precursor. *J. Sol-Gel Sci. Technol.* **2002**, *25*, 121–136. [[CrossRef](#)]
14. Zhang, L.; Gao, C.; Cao, L. The synthesis of nanosized TiO₂ powder using a sol-gel method with TiCl₄ as a precursor. *J. Mater. Sci.* **2000**, *35*, 4049–4054.
15. Ullattil, S.; Periyat, P. Sol-Gel Synthesis of Titanium Dioxide. In *Sol-Gel Materials for Energy, Environment and Electronic Applications. Advances in Sol-Gel Derived Materials and Technologies*; Springer: Cham, Switzerland, 2017; pp. 271–283.
16. Dell'Edera, M.; Petronella, F.; Truppi, A.; Liotta, L.F.; Galli, N.; Sibillano, T.; Giannini, C.; Brescia, R.; Milano, F.; Striccoli, M.; et al. Low Temperature Synthesis of Photocatalytic Mesoporous TiO₂ Nanomaterials. *Catalysts* **2020**, *10*, 893. [[CrossRef](#)]
17. Vargas, M.A.; Rodríguez-Páez, J.E. Facile Synthesis of TiO₂ Nanoparticles of Different Crystalline Phases and Evaluation of Their Antibacterial Effect Under Dark Conditions Against *E. coli*. *J. Clust. Sci.* **2019**, *30*, 379–391. [[CrossRef](#)]
18. Daels, N.; Radoicic, M.; Radetic, M.; De Clerck, K.; Van Hulle, S.W.H. Electrospun nanofibre membranes functionalised with TiO₂ nanoparticles: Evaluation of humic acid and bacterial removal from polluted water. *Sep. Purif. Technol.* **2015**, *149*, 488–494. [[CrossRef](#)]
19. Kim, S.H.; Kwak, S.Y.; Sohn, B.H.; Park, T.H. Design of TiO₂ nanoparticle self-assembled aromatic polyamide thin-film-composite (TFC) membrane as an approach to solve biofouling problem. *J. Membr. Sci.* **2003**, *211*, 157–165. [[CrossRef](#)]
20. Ibrahim, S.A.; Sreekantan, S. Effect of pH on TiO₂ Nanoparticles via Sol-Gel Method. *Adv. Mater. Res.* **2011**, *173*, 184–189. [[CrossRef](#)]

21. Galkina, O.L.; Sycheva, A.; Blagodatskiy, A.; Kaptay, G.; Katanaev, V.L.; Seisenbaeva, G.A.; Kessler, V.G.; Agafonov, A.V. The sol–gel synthesis of cotton/TiO₂ composites and their antibacterial properties. *Surf. Coat. Technol.* **2014**, *253*, 171–179. [[CrossRef](#)]
22. Bahar, M.; Mozaffari, M.; Esmaili, S. Effect of different alcohols, gelatinizing times, calcination and microwave on characteristics of TiO₂ nanoparticles synthesized by sol–gel method. *J. Theoretic. Appl. Phys.* **2017**, *11*, 79–86. [[CrossRef](#)]
23. Duymaz, B.; Yigit, Z.V.; Şeker, M.G.; Dündar, F. Antibacterial Properties of Sol-Gel Derived TiO₂ Nanoparticles. *Acta Phys. Pol. A* **2016**, *129*, 872–874. [[CrossRef](#)]
24. Rasheed, R.; Algawi, S.; Rhoomi, Z. Synthesis and Antibacterial Activity of Rutile-TiO₂ Nano Powder Prepared by Hydrothermal Process. *J. Univ. Babylon Pure Appl. Sci.* **2017**, *25*, 1744–1754.
25. Kőrösi, L.; Prato, M.; Scarpellini, A.; Kovács, J.; Dömötör, D.; Kovács, T.; Papp, S. H₂O₂-assisted photocatalysis on flower-like rutile TiO₂ nanostructures: Rapid dye degradation and inactivation of bacteria. *Appl. Surf. Sci.* **2016**, *365*, 171–179. [[CrossRef](#)]
26. Zárate, R.A.; Fuentes, S.; Wiff, J.P.; Fuenzalida, V.M.; Cabrera, A.L. Chemical composition and phase identification of sodium titanate nanostructures grown from titania by hydrothermal processing. *J. Phys. Chem. Solids* **2007**, *68*, 628–637. [[CrossRef](#)]
27. León-Ríos, S.; Espinoza González, R.; Fuentes, S.; Chávez Ángel, E.; Echeverría, A.; Serrano, A.E.; Demergasso, C.S.; Zárate, R.A. One-Dimensional TiO₂-B Crystals Synthesised by Hydrothermal Process and Their Antibacterial Behaviour on Escherichia coli. *J. Nanomater.* **2016**, *2016*, 7213672. [[CrossRef](#)]
28. Ben-Shahar, Y.; Banin, U. Hybrid Semiconductor–Metal Nanorods as Photocatalysts. *Top. Curr. Chem.* **2016**, *374*, 54. [[CrossRef](#)]
29. Le Ouay, B.; Stellacci, F. Antibacterial activity of silver nanoparticles: A surface science insight. *Nano Today* **2015**, *10*, 339–354. [[CrossRef](#)]
30. Banin, U.; Ben-Shahar, Y.; Vinokurov, K. Hybrid Semiconductor–Metal Nanoparticles: From Architecture to Function. *Chem. Mater.* **2014**, *26*, 97–110. [[CrossRef](#)]
31. Kedziora, A.; Streck, W.; Kepinski, L.; Bugla-Ploskonska, G.; Doroszkiewicz, W. Synthesis and antibacterial activity of novel titanium dioxide doped with silver. *J. Sol-Gel Sci. Technol.* **2012**, *62*, 79–86. [[CrossRef](#)]
32. Carvalho, I.; Ferdov, S.; Mansilla, C.; Marques, S.M.; Cerqueira, M.A.; Pastrana, L.M.; Henriques, M.; Gaidau, C.; Ferreira, P.; Carvalho, S. Development of antimicrobial leather modified with Ag–TiO₂ nanoparticles for footwear industry. *Sci. Technol. Mater.* **2018**, *30*, 60–68. [[CrossRef](#)]
33. Ahmed, A.; Niazi, M.B.K.; Jahan, Z.; Ahmad, T.; Hussain, A.; Pervaiz, E.; Janjua, H.A.; Hussain, Z. In-vitro and in-vivo study of superabsorbent PVA/Starch/g-C₃N₄/Ag@TiO₂ NPs hydrogel membranes for wound dressing. *Eur. Polym. J.* **2020**, *130*, 109650. [[CrossRef](#)]
34. Page, K.; Palgrave, R.G.; Parkin, I.P.; Wilson, M.; Savin, S.L.P.; Chadwick, A.V. Titania and silver–titania composite films on glass—potent antimicrobial coatings. *J. Mater. Chem.* **2007**, *17*, 95–104. [[CrossRef](#)]
35. Amarjargal, A.; Tijjing, L.D.; Ruelo, M.T.G.; Lee, D.H.; Kim, C.S. Facile synthesis and immobilization of Ag–TiO₂ nanoparticles on electrospun PU nanofibers by polyol technique and simple immersion. *Mater. Chem. Phys.* **2012**, *135*, 277–281. [[CrossRef](#)]
36. Skorb, E.V.; Antonouskaya, L.I.; Belyasova, N.A.; Shchukin, D.G.; Möhwald, H.; Sviridov, D.V. Antibacterial activity of thin-film photocatalysts based on metal-modified TiO₂ and TiO₂:In₂O₃ nanocomposite. *Appl. Catal. B* **2008**, *84*, 94–99. [[CrossRef](#)]
37. Kaushik, R.; Samal, P.K.; Halder, A. Degradation of Fluoroquinolone-Based Pollutants and Bacterial Inactivation by Visible-Light-Active Aluminum-Doped TiO₂ Nanoflakes. *ACS Appl. Nano Mater.* **2019**, *2*, 7898–7909. [[CrossRef](#)]
38. Venieri, D.; Gounaki, I.; Bikouvaraki, M.; Binas, V.; Zachopoulos, A.; Kiriakidis, G.; Mantzavinos, D. Solar photocatalysis as disinfection technique: Inactivation of Klebsiella pneumoniae in sewage and investigation of changes in antibiotic resistance profile. *J. Environ. Manag.* **2017**, *195*, 140–147. [[CrossRef](#)]
39. Binas, V.D.; Sambani, K.; Maggos, T.; Katsanaki, A.; Kiriakidis, G. Synthesis and photocatalytic activity of Mn-doped TiO₂ nanostructured powders under UV and visible light. *Appl. Catal. B* **2012**, *113–114*, 79–86. [[CrossRef](#)]
40. Venieri, D.; Fraggadaki, A.; Kostadima, M.; Chatzisyneon, E.; Binas, V.; Zachopoulos, A.; Kiriakidis, G.; Mantzavinos, D. Solar light and metal-doped TiO₂ to eliminate water-transmitted bacterial pathogens: Photocatalyst characterization and disinfection performance. *Appl. Catal. B* **2014**, *154–155*, 93–101. [[CrossRef](#)]

41. Hassan, M.S.; Amna, T.; Yang, O.B.; Kim, H.-C.; Khil, M.-S. TiO₂ nanofibers doped with rare earth elements and their photocatalytic activity. *Ceram. Int.* **2012**, *38*, 5925–5930. [[CrossRef](#)]
42. Nithya, N.; Bhoopathi, G.; Magesh, G.; Kumar, C.D.N. Neodymium doped TiO₂ nanoparticles by sol-gel method for antibacterial and photocatalytic activity. *Mater. Sci. Semicond. Process* **2018**, *83*, 70–82. [[CrossRef](#)]
43. Siwińska-Stefańska, K.; Kubiak, A.; Piasecki, A.; Dobrowolska, A.; Czaczyk, K.; Motylenko, M.; Rafaja, D.; Ehrlich, H.; Jesionowski, T. Hydrothermal synthesis of multifunctional TiO₂-ZnO oxide systems with desired antibacterial and photocatalytic properties. *Appl. Surf. Sci.* **2019**, *463*, 791–801. [[CrossRef](#)]
44. Liu, Y.; Zeng, X.K.; Hu, X.Y.; Hu, J.; Wang, Z.Y.; Yin, Y.C.; Sun, C.H.; Zhang, X.W. Two-dimensional g-C₃N₄/TiO₂ nanocomposites as vertical Z-scheme heterojunction for improved photocatalytic water disinfection. *Catal. Today* **2019**, *335*, 243–251. [[CrossRef](#)]
45. Sikora, P.; Cendrowski, K.; Markowska-Szczupak, A.; Horszczaruk, E.; Mijowska, E. The effects of silica/titania nanocomposite on the mechanical and bactericidal properties of cement mortars. *Constr. Build. Mater.* **2017**, *150*, 738–746. [[CrossRef](#)]
46. Wu, Q.; Zhang, Z.H. The Fabrication of Magnetically Recyclable La-Doped TiO₂/Calcium Ferrite/Diatomite Composite for Visible-Light-Driven Degradation of Antibiotic and Disinfection of Bacteria. *Environ. Eng. Sci.* **2020**, *37*, 109–119. [[CrossRef](#)]
47. Xu, W.R.; Xie, W.J.; Huang, X.Q.; Chen, X.; Huang, N.; Wang, X.; Liu, J. The graphene oxide and chitosan biopolymer loads TiO₂ for antibacterial and preservative research. *Food Chem.* **2017**, *221*, 267–277. [[CrossRef](#)]
48. Ghosh, M.; Mondal, M.; Mandal, S.; Roy, A.; Chakrabarty, S.; Chakrabarti, G.; Pradhan, S.K. Enhanced photocatalytic and antibacterial activities of mechanosynthesized TiO₂-Ag nanocomposite in wastewater treatment. *J. Mol. Struct.* **2020**, *1211*, 11. [[CrossRef](#)]
49. Liga, M.V.; Bryant, E.L.; Colvin, V.L.; Li, Q.L. Virus inactivation by silver doped titanium dioxide nanoparticles for drinking water treatment. *Water Res.* **2011**, *45*, 535–544. [[CrossRef](#)]
50. Xiao, G.; Zhang, X.; Zhang, W.Y.; Zhang, S.; Su, H.J.; Tan, T.W. Visible-light-mediated synergistic photocatalytic antimicrobial effects and mechanism of Ag-nanoparticles@chitosan-TiO₂ organic-inorganic composites for water disinfection. *Appl. Catal. B-Environ.* **2015**, *170*, 255–262. [[CrossRef](#)]
51. Haghghat, N.; Vatanpour, V.; Sheydaei, M.; Nikjavan, Z. Preparation of a novel polyvinyl chloride (PVC) ultrafiltration membrane modified with Ag/TiO₂ nanoparticle with enhanced hydrophilicity and antibacterial activities. *Sep. Purif. Technol.* **2020**, *237*, 116374. [[CrossRef](#)]
52. Kim, B.C.; Jeong, E.; Kim, E.; Hong, S.W. Bio-organic-inorganic hybrid photocatalyst, TiO₂ and glucose oxidase composite for enhancing antibacterial performance in aqueous environments. *Appl. Catal., B* **2019**, *242*, 194–201. [[CrossRef](#)]
53. Monmatrapoj, N.; Sri-On, A.; Klinsukhon, W.; Boonnak, K.; Prahsarn, C. Antiviral activity of multifunctional composite based on TiO₂-modified hydroxyapatite. *Mater. Sci. Eng. C Mater. Biol. Appl.* **2018**, *92*, 96–102. [[CrossRef](#)] [[PubMed](#)]
54. Li, T.; Xiao, Y.R.; Guo, D.X.; Shen, L.G.; Li, R.J.; Jiao, Y.; Xu, Y.C.; Lin, H.J. In-situ coating TiO₂ surface by plant-inspired tannic acid for fabrication of thin film nanocomposite nanofiltration membranes toward enhanced separation and antibacterial performance. *J. Colloid Interface Sci.* **2020**, *572*, 114–121. [[CrossRef](#)] [[PubMed](#)]
55. Lin, X.; Li, J.; Ma, S.; Liu, G.; Yang, K.; Tong, M.; Lin, D. Toxicity of TiO₂ Nanoparticles to Escherichia coli: Effects of Particle Size, Crystal Phase and Water Chemistry. *PLoS ONE* **2014**, *9*, e110247. [[CrossRef](#)]
56. Shirai, R.; Miura, T.; Yoshida, A.; Yoshino, F.; Ito, T.; Yoshinari, M.; Yajima, Y. Antimicrobial effect of titanium dioxide after ultraviolet irradiation against periodontal pathogen. *Dent. Mater. J.* **2016**, *35*, 511–516. [[CrossRef](#)]
57. Rtimi, S.; Giannakis, S.; Bensimon, M.; Pulgarin, C.; Sanjines, R.; Kiwi, J. Supported TiO₂ films deposited at different energies: Implications of the surface compactness on the catalytic kinetics. *Appl. Catal. B* **2016**, *191*, 42–52. [[CrossRef](#)]
58. Sunada, K.; Kikuchi, Y.; Hashimoto, K.; Fujishima, A. Bactericidal and Detoxification Effects of TiO₂ Thin Film Photocatalysts. *Environ. Sci. Technol.* **1998**, *32*, 726–728. [[CrossRef](#)]
59. Wang, W.; Li, G.; Xia, D.; An, T.; Zhao, H.; Wong, P.K. Photocatalytic nanomaterials for solar-driven bacterial inactivation: Recent progress and challenges. *Environ. Sci. Nano* **2017**, *4*, 782–799. [[CrossRef](#)]
60. Wang, M.; Zhao, Q.; Yang, H.; Shi, D.; Qian, J. Photocatalytic antibacterial properties of copper doped TiO₂ prepared by high-energy ball milling. *Ceram. Int.* **2020**, *46*, 16716–16724. [[CrossRef](#)]

61. Ren, Y.; Han, Y.; Li, Z.; Liu, X.; Zhu, S.; Liang, Y.; Yeung, K.W.K.; Wu, S. Ce and Er Co-doped TiO₂ for rapid bacteria-killing using visible light. *Bioact. Mater.* **2020**, *5*, 201–209. [[CrossRef](#)]
62. Liu, N.; Zhu, Q.; Zhang, N.; Zhang, C.; Kawazoe, N.; Chen, G.; Negishi, N.; Yang, Y. Superior disinfection effect of Escherichia coli by hydrothermal synthesized TiO₂-based composite photocatalyst under LED irradiation: Influence of environmental factors and disinfection mechanism. *Environ. Pollut.* **2019**, *247*, 847–856. [[CrossRef](#)] [[PubMed](#)]
63. Silhavy, T.J.; Kahne, D.; Walker, S. The bacterial cell envelope. *Cold Spring Harb. Perspect. Biol.* **2010**, *2*, a000414. [[CrossRef](#)] [[PubMed](#)]
64. Nikaido, H. Molecular basis of bacterial outer membrane permeability revisited. *Microbiol. Mol. Biol. Rev.* **2003**, *67*, 593–656. [[CrossRef](#)]
65. Wang, L.; Hu, C.; Shao, L. The antimicrobial activity of nanoparticles: Present situation and prospects for the future. *Int. J. Nanomed.* **2017**, *12*, 1227–1249. [[CrossRef](#)] [[PubMed](#)]
66. Fu, G.; Vary, P.S.; Lin, C.-T. Anatase TiO₂ Nanocomposites for Antimicrobial Coatings. *J. Phys. Chem. B* **2005**, *109*, 8889–8898. [[CrossRef](#)]
67. Alizadeh Sani, M.; Ehsani, A.; Hashemi, M. Whey protein isolate/cellulose nanofibre/TiO₂ nanoparticle/rosemary essential oil nanocomposite film: Its effect on microbial and sensory quality of lamb meat and growth of common foodborne pathogenic bacteria during refrigeration. *Int. J. Food. Microbiol.* **2017**, *251*, 8–14. [[CrossRef](#)]
68. Nakano, R.; Hara, M.; Ishiguro, H.; Yao, Y.; Ochiai, T.; Nakata, K.; Murakami, T.; Kajioka, J.; Sunada, K.; Hashimoto, K.; et al. Broad Spectrum Microbicidal Activity of Photocatalysis by TiO₂. *Catalysts* **2013**, *3*, 310–323. [[CrossRef](#)]
69. Backhaus, K.; Marugan, J.; van Grieken, R.; Sordo, C. Photocatalytic inactivation of *E. faecalis* in secondary wastewater plant effluents. *Water. Sci. Technol.* **2010**, *61*, 2355–2361. [[CrossRef](#)]
70. Pal, A.; Pehkonen, S.O.; Yu, L.E.; Ray, M.B. Photocatalytic inactivation of Gram-positive and Gram-negative bacteria using fluorescent light. *J. Photochem. Photobiol. A* **2007**, *186*, 335–341. [[CrossRef](#)]
71. Ripolles-Avila, C.; Martinez-Garcia, M.; Hascoët, A.-S.; Rodríguez-Jerez, J.J. Bactericidal efficacy of UV activated TiO₂ nanoparticles against Gram-positive and Gram-negative bacteria on suspension. *J. Food* **2019**, *17*, 408–418. [[CrossRef](#)]
72. Tsuang, Y.H.; Sun, J.S.; Huang, Y.C.; Lu, C.H.; Chang, W.H.; Wang, C.C. Studies of photokilling of bacteria using titanium dioxide nanoparticles. *Artif. Organs.* **2008**, *32*, 167–174. [[CrossRef](#)] [[PubMed](#)]
73. van Grieken, R.; Marugán, J.; Pablos, C.; Furones, L.; López, A. Comparison between the photocatalytic inactivation of Gram-positive *E. faecalis* and Gram-negative *E. coli* faecal contamination indicator microorganisms. *Appl. Catal. B* **2010**, *100*, 212–220. [[CrossRef](#)]
74. Haider, A.J.; AL-Anbar, R.H.; Kadhim, G.R.; Salame, C.T. Exploring potential Environmental applications of TiO₂ Nanoparticles. *Energy Proc.* **2017**, *119*, 332–345. [[CrossRef](#)]
75. Rincón, A.-G.; Pulgarin, C. Bactericidal action of illuminated TiO₂ on pure Escherichia coli and natural bacterial consortia: Post-irradiation events in the dark and assessment of the effective disinfection time. *Appl. Catal. B* **2004**, *49*, 99–112. [[CrossRef](#)]
76. Child, M.; Strike, P.; Pickup, R.; Edwards, C. Salmonella typhimurium displays cyclical patterns of sensitivity to UV-C killing during prolonged incubation in the stationary phase of growth. *FEMS Microbiol. Lett.* **2002**, *213*, 81–85. [[CrossRef](#)]
77. Munro, P.M.; Flatau, G.N.; Clément, R.L.; Gauthier, M.J. Influence of the RpoS (KatF) sigma factor on maintenance of viability and culturability of Escherichia coli and Salmonella typhimurium in seawater. *Appl. Environ. Microbiol.* **1995**, *61*, 1853. [[CrossRef](#)]
78. Eisenstark, A.; Calcutt, M.J.; Becker-Hapak, M.; Ivanova, A. Role of escherichia coli rpos and associated genes in defense against oxidative damage. *Free Radic. Biol. Med.* **1996**, *21*, 975–993. [[CrossRef](#)]
79. Prieto-Calvo, M.A.; López, M.; Prieto, M.; Alvarez-Ordóñez, A. Variability in resistance to Cold Atmospheric Plasma (CAP) and Ultraviolet light (UV) and multiple stress resistance analysis of pathogenic verocytotoxigenic Escherichia coli (VTEC). *Food Res. Int.* **2016**, *79*, 88–94. [[CrossRef](#)]
80. Janulczyk, R.; Ricci, S.; Bjorck, L. MtsABC is important for manganese and iron transport, oxidative stress resistance, and virulence of Streptococcus pyogenes. *Infect. Immun.* **2003**, *71*, 2656–2664. [[CrossRef](#)]
81. Mandel, G.L. Catalase, superoxide dismutase, and virulence of Staphylococcus aureus. In vitro and in vivo studies with emphasis on staphylococcal-leukocyte interaction. *J. Clin. Investig.* **1975**, *55*, 561–566. [[CrossRef](#)]

82. Rodriguez-Gonzalez, V.; Obregon, S.; Patron-Soberano, O.A.; Terashima, C.; Fujishima, A. An approach to the photocatalytic mechanism in the TiO₂-nanomaterials microorganism interface for the control of infectious processes. *Appl. Catal. B* **2020**, *270*, 118853. [[CrossRef](#)]
83. Bonnet, M.; Massard, C.; Veisseire, P.; Camares, O.; Awitor, K.O. Environmental Toxicity and Antimicrobial Efficiency of Titanium Dioxide Nanoparticles in Suspension. *J. Biomater. Nanobiotechnol.* **2015**, *06*, 213–224. [[CrossRef](#)]
84. Pagnout, C.; Jomini, S.; Dadhwal, M.; Caillet, C.; Thomas, F.; Bauda, P. Role of electrostatic interactions in the toxicity of titanium dioxide nanoparticles toward Escherichia coli. *Colloids Surf. B Biointerfaces* **2012**, *92*, 315–321. [[CrossRef](#)]
85. Adams, L.K.; Lyon, D.Y.; Alvarez, P.J. Comparative eco-toxicity of nanoscale TiO₂, SiO₂, and ZnO water suspensions. *Water Res* **2006**, *40*, 3527–3532. [[CrossRef](#)]
86. Nestic, J.; Rtimi, S.; Laub, D.; Roglic, G.M.; Pulgarin, C.; Kiwi, J. New evidence for TiO₂ uniform surfaces leading to complete bacterial reduction in the dark: Critical issues. *Colloids Surf. B Biointerfaces* **2014**, *123*, 593–599. [[CrossRef](#)]
87. Kiwi, J.; Rtimi, S.; Sanjines, R.; Pulgarin, C. TiO₂ and TiO₂-Doped Films Able to Kill Bacteria by Contact: New Evidence for the Dynamics of Bacterial Inactivation in the Dark and under Light Irradiation. *Int. J. Photoenergy* **2014**, *2014*, 785037. [[CrossRef](#)]
88. Rtimi, S.; Nestic, J.; Pulgarin, C.; Sanjines, R.; Bensimon, M.; Kiwi, J. Effect of surface pretreatment of TiO₂ films on interfacial processes leading to bacterial inactivation in the dark and under light irradiation. *Interface Focus* **2015**, *5*, 20140046. [[CrossRef](#)]
89. Erdem, A.; Metzler, D.; Cha, D.; Huang, C.P. Inhibition of bacteria by photocatalytic nano-TiO₂ particles in the absence of light. *Int. J. Environ. Sci. Technol.* **2014**, *12*, 2987–2996. [[CrossRef](#)]
90. Carré, G.; Hamon, E.; Ennahar, S.; Estner, M.; Lett, M.C.; Horvatovich, P.; Gies, J.P.; Keller, V.; Keller, N.; Andre, P. TiO₂ photocatalysis damages lipids and proteins in Escherichia coli. *Appl. Environ. Microbiol.* **2014**, *80*, 2573–2581. [[CrossRef](#)]
91. Sułek, A.; Pucelik, B.; Kuncewicz, J.; Dubin, G.; Dąbrowski, J.M. Sensitization of TiO₂ by halogenated porphyrin derivatives for visible light biomedical and environmental photocatalysis. *Catal. Today* **2019**, *335*, 538–549. [[CrossRef](#)]
92. Gibson, K.E. Viral pathogens in water: Occurrence, public health impact, and available control strategies. *Curr. Opin. Virol.* **2014**, *4*, 50–57. [[CrossRef](#)]
93. Otter, J.A.; Yezli, S.; Salkeld, J.A.; French, G.L. Evidence that contaminated surfaces contribute to the transmission of hospital pathogens and an overview of strategies to address contaminated surfaces in hospital settings. *Am. J. Infect. Control* **2013**, *41*, S6–S11. [[CrossRef](#)]
94. Barker, J.; Vipond, I.B.; Bloomfield, S.F. Effects of cleaning and disinfection in reducing the spread of Norovirus contamination via environmental surfaces. *J. Hosp. Infect.* **2004**, *58*, 42–49. [[CrossRef](#)]
95. Kramer, A.; Schwebke, I.; Kampf, G. How long do nosocomial pathogens persist on inanimate surfaces? A systematic review. *BMC Infect. Dis.* **2006**, *6*, 130. [[CrossRef](#)]
96. Li, Q.; Page, M.; Marinas, B.J.; Ahang, F.K. Treatment of Coliphage MS2 with Palladium-Modified Nitrogen-Doped Titanium Oxide Photocatalyst Illuminated by Visible Light. *Environ. Sci. Technol.* **2008**, *42*, 6148–6153. [[CrossRef](#)]
97. Syngouna, V.I.; Chrysikopoulos, C.V. Inactivation of MS2 bacteriophage by titanium dioxide nanoparticles in the presence of quartz sand with and without ambient light. *J. Colloid Interface Sci.* **2017**, *497*, 117–125. [[CrossRef](#)]
98. Koizumi, Y.; Taya, M. Kinetic evaluation of biocidal activity of titanium dioxide against phage MS2 considering interaction between the phage and photocatalyst particles. *Biochem. Eng. J.* **2002**, *12*, 107–116. [[CrossRef](#)]
99. Ditta, I.B.; Steele, A.; Liptrot, C.; Tobin, J.; Tyler, H.; Yates, H.M.; Sheel, D.W.; Foster, H.A. Photocatalytic antimicrobial activity of thin surface films of TiO₂, CuO and TiO₂/CuO dual layers on Escherichia coli and bacteriophage T4. *Appl. Microbiol. Biotechnol.* **2008**, *79*, 127–133. [[CrossRef](#)]
100. Ishiguro, H.; Nakano, R.; Yao, Y.; Kajioaka, J.; Fujishima, A.; Sunada, K.; Minoshima, M.; Hashimoto, K.; Kubota, Y. Photocatalytic inactivation of bacteriophages by TiO₂-coated glass plates under low-intensity, long-wavelength UV irradiation. *Photochem. Photobiol. Sci.* **2011**, *10*, 1825–1829. [[CrossRef](#)]

101. Ishiguro, H.; Yao, Y.; Nakano, R.; Hara, M.; Sunada, K.; Hashimoto, K.; Kajioka, J.; Fujishima, A.; Kubota, Y. Photocatalytic activity of Cu²⁺/TiO₂-coated cordierite foam inactivates bacteriophages and Legionella pneumophila. *Appl. Catal. B* **2013**, *129*, 56–61. [[CrossRef](#)]
102. Soylemez, E.; de Boer, M.P.; Sae-Ueng, U.; Evilevitch, A.; Stewart, T.A.; Nyman, M. Photocatalytic Degradation of Bacteriophages Evidenced by Atomic Force Microscopy. *PLoS ONE* **2013**, *8*, e53601. [[CrossRef](#)]
103. Gerrity, D.; Ryu, H.; Crittenden, J.; Abbaszadegan, M. Photocatalytic inactivation of viruses using titanium dioxide nanoparticles and low-pressure UV light. *J. Environ. Sci. Health Part A Toxic/Hazard. Subst. Environ. Eng.* **2008**, *43*, 1261–1270. [[CrossRef](#)]
104. Hajkova, P.; Spatenka, P.; Horsky, J.; Horska, I.; Kolouch, A. Photocatalytic Effect of TiO₂ Films on Viruses and Bacteria. *Plasma Processes Polym.* **2007**, *4*, S397–S401. [[CrossRef](#)]
105. Nakano, R.; Ishiguro, H.; Yao, Y.; Kajioka, J.; Fujishima, A.; Sunada, K.; Minoshima, M.; Hashimoto, K.; Kubota, Y. Photocatalytic inactivation of influenza virus by titanium dioxide thin film. *Photochem. Photobiol. Sci.* **2012**, *11*, 1293–1298. [[CrossRef](#)]
106. Guillard, C.; Bui, T.H.; Felix, C.; Moules, V.; Lina, B.; Lejeune, P. Microbiological disinfection of water and air by photocatalysis. *C. R. Chim.* **2008**, *11*, 107–113. [[CrossRef](#)]
107. Mazurkova, N.A.; Spitsyna, Y.E.; Shikina, N.V.; Ismagilov, Z.R.; Zagrebel'nyi, S.N.; Ryabchikova, E.I. Interaction of titanium dioxide nanoparticles with influenza virus. *Nanotechnol. Russia* **2010**, *5*, 417–420. [[CrossRef](#)]
108. Zheng, X.; Shen, Z.-p.; Cheng, C.; Shi, L.; Cheng, R.; Yuan, D.-H. Photocatalytic disinfection performance in virus and virus/bacteria system by Cu-TiO₂ nanofibers under visible light. *Environ. Pollut.* **2018**, *237*, 452–459. [[CrossRef](#)]
109. Bintsis, T.; Litopoulou-Tzanetaki, E.; Robinson, R.K. Existing and potential applications of ultraviolet light in the food industry—a critical review. *J. Sci. Food Agric.* **2000**, *80*, 637–645. [[CrossRef](#)]
110. Xu, R.; Liu, X.; Zhang, P.; Ma, H.; Liu, G.; Xia, Z. The photodestruction of virus in Nano-TiO₂ suspension. *J. Wuhan Univ. Technol. Mater. Sci. Ed.* **2007**, *22*, 422–425. [[CrossRef](#)]
111. Liga, M.V.; Maguire-Boyle, S.J.; Jafry, H.R.; Barron, A.R.; Li, Q. Silica decorated TiO₂ for virus inactivation in drinking water—simple synthesis method and mechanisms of enhanced inactivation kinetics. *Environ. Sci. Technol.* **2013**, *47*, 6463–6470. [[CrossRef](#)]
112. Fiorillo, L.; Cervino, G.; Matarese, M.; D'Amico, C.; Surace, G.; Paduano, V.; Fiorillo, M.T.; Moschella, A.; Bruna, A.; Romano, G.L.; et al. COVID-19 Surface Persistence: A Recent Data Summary and Its Importance for Medical and Dental Settings. *Int. J. Environ. Res. Public Health* **2020**, *17*, 3132. [[CrossRef](#)] [[PubMed](#)]
113. Khaiboullina, S.; Uppal, T.; Dhabarde, N.; Subramanian, V.R.; Verma, S.C. In Vitro Inactivation of Human Coronavirus by Titania Nanoparticle Coatings and UVC Radiation: Throwing Light on SARS-CoV-2. *bioRxiv* **2020**. [[CrossRef](#)]
114. Seven, O.; Dindar, B.; Aydemir, S.; Metin, D.; Ozinel, M.A.; Icli, S. Solar photocatalytic disinfection of a group of bacteria and fungi aqueous suspensions with TiO₂, ZnO and Sahara desert dust. *J. Photochem. Photobiol. A* **2004**, *165*, 103–107. [[CrossRef](#)]
115. Maneerat, C.; Hayata, Y. Antifungal activity of TiO₂ photocatalysis against *Penicillium expansum* in vitro and in fruit tests. *Int. J. Food. Microbiol.* **2006**, *107*, 99–103. [[CrossRef](#)]
116. Polo-López, M.I.; Fernández-Ibáñez, P.; García-Fernández, I.; Oller, I.; Salgado-Tránsito, I.; Sichel, C. Resistance of *Fusarium* sp spores to solar TiO₂ photocatalysis: Influence of spore type and water (scaling-up results). *J. Chem. Technol. Biotechnol.* **2010**, *85*, 1038–1048. [[CrossRef](#)]
117. Sichel, C.; Tello, J.; de Cara, M.; Fernández-Ibáñez, P. Effect of UV solar intensity and dose on the photocatalytic disinfection of bacteria and fungi. *Catal. Today* **2007**, *129*, 152–160. [[CrossRef](#)]
118. Sichel, C.; de Cara, M.; Tello, J.; Blanco, J.; Fernández-Ibáñez, P. Solar photocatalytic disinfection of agricultural pathogenic fungi: *Fusarium* species. *Appl. Catal. B* **2007**, *74*, 152–160. [[CrossRef](#)]
119. Hochmannova, L.; Vytrasova, J. Photocatalytic and antimicrobial effects of interior paints. *Prog. Org. Coat.* **2010**, *67*, 1–5. [[CrossRef](#)]
120. Muranyi, P.; Schraml, C.; Wunderlich, J. Antimicrobial efficiency of titanium dioxide-coated surfaces. *J. Appl. Microbiol.* **2010**, *108*, 1966–1973. [[CrossRef](#)]
121. Vucetic, S.B.; Rudic, O.; Markov, S.L.; Bera, O.J.; Vidakovic, A.M.; Skapin, A.S.; Ranogajec, J.G. Antifungal efficiency assessment of the TiO₂ coating on facade paints. *Environ. Sci. Pollut. Res. Int.* **2014**, *21*, 11228–11237. [[CrossRef](#)]

122. Lonnen, J.; Kilvington, S.; Kehoe, S.C.; Al-Touati, F.; McGuigan, K.G. Solar and photocatalytic disinfection of protozoan, fungal and bacterial microbes in drinking water. *Water Res.* **2005**, *39*, 877–883. [[CrossRef](#)] [[PubMed](#)]
123. Kühn, K.P.; Chaberny, I.F.; Massholder, K.; Stickler, M.; Benz, V.W.; Sonntag, H.-G.; Erdinger, L. Disinfection of surfaces by photocatalytic oxidation with titanium dioxide and UVA light. *Chemosphere* **2003**, *53*, 71–77. [[CrossRef](#)]
124. Ohara, T.; Tsuge, T. FoSTUA, encoding a basic helix-loop-helix protein, differentially regulates development of three kinds of asexual spores, macroconidia, microconidia, and chlamydospores, in the fungal plant pathogen *Fusarium oxysporum*. *Eukaryot. Cell* **2004**, *3*, 1412–1422. [[CrossRef](#)]
125. Negishi, N.; Miyazaki, Y.; Kato, S.; Yang, Y. Effect of HCO_3^- concentration in groundwater on TiO_2 photocatalytic water purification. *Appl. Catal. B* **2019**, *242*, 449–459. [[CrossRef](#)]
126. Guillard, C.; Puzenat, E.; Lachheb, H.; Houas, A.; Herrmann, J.-M. Why inorganic salts decrease the TiO_2 photocatalytic efficiency. *Int. J. Photoenergy* **2005**, *7*, 641208. [[CrossRef](#)]
127. Pratap Reddy, M.; Venugopal, A.; Subrahmanyam, M. Hydroxyapatite-supported Ag- TiO_2 as *Escherichia coli* disinfection photocatalyst. *Water Res.* **2007**, *41*, 379–386. [[CrossRef](#)] [[PubMed](#)]
128. ISO27447:2019. *Fine Ceramics (Advanced Ceramics, Advanced Technical Ceramics)—Test Method for Antibacterial Activity of Semiconducting Photocatalytic Materials*; International Organization for Standardization: Geneva, Switzerland, 2019.
129. JISR1702:2012. *Fine Ceramics (Advanced Ceramics, Advanced Technical Ceramics)—Test Method For Antibacterial Activity of Photocatalytic Products under Photoirradiation and Efficacy*; Japanese Standards Association, 2012.
130. ISO18061:2014. *Fine Ceramics (Advanced Ceramics, Advanced Technical Ceramics)—Determination of Antiviral Activity of Semiconducting Photocatalytic Materials—Test Method Using Bacteriophage Q-Beta*; International Organization for Standardization: Geneva, Switzerland, 2014.
131. JISR1706:2013. *Fine Ceramics (Advanced Ceramics, Advanced Technical Ceramics)—Determination of Antiviral Activity of Photocatalytic Materials—Test Method Using Bacteriophage Q-Beta*; Japanese Standard Association, 2013.
132. ISO13125:2013. *Fine Ceramics (Advanced Ceramics, Advanced Technical Ceramics)—Test Method for Antifungal Activity of Semiconducting Photocatalytic Materials*; International Organization for Standardization, 2013.
133. JISR1705:2016. *Fine Ceramics (Advanced Ceramics, Advanced Technical Ceramics)—Test Method for Antifungal Activity of Photocatalytic Products under Photoirradiation*; Japanese Standard Association, 2016.
134. Karagoz, S.; Kiremitler, N.B.; Sakir, M.; Salem, S.; Onses, M.S.; Sahmetlioglu, E.; Ceylan, A.; Yilmaz, E. Synthesis of Ag and TiO_2 modified polycaprolactone electrospun nanofibers (PCL/ TiO_2 -Ag NFs) as a multifunctional material for SERS, photocatalysis and antibacterial applications. *Ecotoxicol. Environ. Saf.* **2020**, *188*, 109856. [[CrossRef](#)]
135. Lei, S.; Guo, G.; Xiong, B.; Gong, W.; Mei, G. Disruption of bacterial cells by photocatalysis of montmorillonite supported titanium dioxide. *J. Wuhan Univ. Technol. Mater. Sci. Ed.* **2009**, *24*, 557–561. [[CrossRef](#)]
136. Abdelbasir, S.M.; Shalan, A.E. An overview of nanomaterials for industrial wastewater treatment. *Korean J. Chem. Eng.* **2019**, *36*, 1209–1225. [[CrossRef](#)]
137. Akpan, U.G.; Hameed, B.H. Parameters affecting the photocatalytic degradation of dyes using TiO_2 -based photocatalysts: A review. *J. Hazard. Mater.* **2009**, *170*, 520–529. [[CrossRef](#)]
138. Reddy, P.V.; Kim, K.H. A review of photochemical approaches for the treatment of a wide range of pesticides. *J. Hazard. Mater.* **2015**, *285*, 325–335. [[CrossRef](#)] [[PubMed](#)]
139. Truppi, A.; Petronella, F.; Placido, T.; Margiotta, V.; Lasorella, G.; Giotta, L.; Giannini, C.; Sibillano, T.; Murgolo, S.; Mascolo, G.; et al. Gram-scale synthesis of UV-vis light active plasmonic photocatalytic nanocomposite based on TiO_2/Au nanorods for degradation of pollutants in water. *Appl. Catal. B* **2019**, *243*, 604–613. [[CrossRef](#)]
140. Tahir, M.B.; Ahmad, A.; Iqbal, T.; Ijaz, M.; Muhammad, S.; Siddeeg, S.M. Advances in photo-catalysis approach for the removal of toxic personal care product in aqueous environment. *Environ. Dev. Sustain.* **2020**, *22*, 6029–6052. [[CrossRef](#)]
141. Zhang, G.; Li, W.; Chen, S.; Zhou, W.; Chen, J. Problems of conventional disinfection and new sterilization methods for antibiotic resistance control. *Chemosphere* **2020**, *254*, 126831. [[CrossRef](#)] [[PubMed](#)]
142. Mahendra, S.; Li, Q.L.; Lyon, D.Y.; Brunet, L.; Alvarez, P.J.J. *Nanotechnology-Enabled Water Disinfection and Microbial Control: Merits and Limitations*; William Andrew Inc.: Norwich, UK, 2009; pp. 157–166.

143. Mascolo, G.; Comparelli, R.; Curri, M.L.; Lovecchio, G.; Lopez, A.; Agostiano, A. Photocatalytic degradation of methyl red by TiO₂: Comparison of the efficiency of immobilized nanoparticles versus conventional suspended catalyst. *J. Hazard. Mater.* **2007**, *142*, 130–137. [[CrossRef](#)] [[PubMed](#)]
144. Bianculllo, F.; Moreira, N.F.F.; Ribeiro, A.R.; Manaia, C.M.; Faria, J.L.; Nunes, O.C.; Castro-Silva, S.M.; Silva, A.M.T. Heterogeneous photocatalysis using UVA-LEDs for the removal of antibiotics and antibiotic resistant bacteria from urban wastewater treatment plant effluents. *Chem. Eng. J.* **2019**, *367*, 304–313. [[CrossRef](#)]
145. Rizzo, L.; Sannino, D.; Vaiano, V.; Sacco, O.; Scarpa, A.; Pietrogiamomi, D. Effect of solar simulated N-doped TiO₂ photocatalysis on the inactivation and antibiotic resistance of an *E. coli* strain in biologically treated urban wastewater. *Appl. Catal. B* **2014**, *144*, 369–378. [[CrossRef](#)]
146. Rizzo, L.; Della Sala, A.; Fiorentino, A.; Puma, G.L. Disinfection of urban wastewater by solar driven and UV lamp-TiO₂ photocatalysis: Effect on a multi drug resistant *Escherichia coli* strain. *Water Res.* **2014**, *53*, 145–152. [[CrossRef](#)]
147. Li, H.Z.; Shen, L.Y.; Zhang, K.F.; Sun, B.J.; Ren, L.P.; Qiao, P.Z.; Pan, K.; Wang, L.; Zhou, W. Surface plasmon resonance-enhanced solar-driven photocatalytic performance from Ag nanoparticle-decorated self-floating porous black TiO₂ foams. *Appl. Catal. B* **2018**, *220*, 111–117. [[CrossRef](#)]
148. Negishi, N.; Chawengkijwanich, C.; Pimpha, N.; Larpkittaworn, S.; Charinpanitkul, T. Performance verification of the photocatalytic solar water purification system for sterilization using actual drinking water in Thailand. *J. Water Process Eng.* **2019**, *31*, 100835. [[CrossRef](#)]
149. Colmenares, J.C.; Kuna, E. Photoactive Hybrid Catalysts Based on Natural and Synthetic Polymers: A Comparative Overview. *Molecules* **2017**, *22*, 790. [[CrossRef](#)] [[PubMed](#)]
150. Castro-Munoz, R. The Role of New Inorganic Materials in Composite Membranes for Water Disinfection. *Membranes* **2020**, *10*, 101. [[CrossRef](#)] [[PubMed](#)]
151. Zheng, X.; Shen, Z.P.; Shi, L.; Cheng, R.; Yuan, D.H. Photocatalytic Membrane Reactors (PMRs) in Water Treatment: Configurations and Influencing Factors. *Catalysts* **2017**, *7*, 224. [[CrossRef](#)]
152. Riaz, S.; Park, S.-J. An overview of TiO₂-based photocatalytic membrane reactors for water and wastewater treatments. *J. Ind. Eng. Chem.* **2020**, *84*, 23–41. [[CrossRef](#)]
153. Cheng, R.; Shen, L.J.; Wang, Q.; Xiang, S.Y.; Shi, L.; Zheng, X.; Lv, W.Z. Photocatalytic Membrane Reactor (PMR) for Virus Removal in Drinking Water: Effect of Humic Acid. *Catalysts* **2018**, *8*, 284. [[CrossRef](#)]
154. Jiang, L.; Zhang, X.; Choo, K.-H. Submerged microfiltration-catalysis hybrid reactor treatment: Photocatalytic inactivation of bacteria in secondary wastewater effluent. *Sep. Purif. Technol.* **2018**, *198*, 87–92. [[CrossRef](#)]
155. Liu, L.; Liu, Z.Y.; Bai, H.W.; Sun, D.D. Concurrent filtration and solar photocatalytic disinfection/degradation using high-performance Ag/TiO₂ nanofiber membrane. *Water Res.* **2012**, *46*, 1101–1112. [[CrossRef](#)]
156. Ishikawa, T.; Yamaoka, H.; Harada, Y.; Fujii, T.; Nagasawa, T. A general process for in situ formation of functional surface layers on ceramics. *Nature* **2002**, *416*, 64–67. [[CrossRef](#)]
157. Nazerah, A.; Ismail, A.F.; Jaafar, J. Incorporation of bactericidal nanomaterials in development of antibacterial membrane for biofouling mitigation: A mini review. *J. Teknol.* **2016**, *78*, 53–61. [[CrossRef](#)]
158. Donlan, R.M. Biofilms: Microbial life on surfaces. *Emerg. Infect. Dis.* **2002**, *8*, 881–890. [[CrossRef](#)]
159. Sotto, A.; Boromand, A.; Zhang, R.X.; Luis, P.; Arsuaga, J.M.; Kim, J.; Van der Bruggen, B. Effect of nanoparticle aggregation at low concentrations of TiO₂ on the hydrophilicity, morphology, and fouling resistance of PES-TiO₂ membranes. *J. Colloid Interface Sci.* **2011**, *363*, 540–550. [[CrossRef](#)]
160. Becerra, J.; Zaderenko, A.P.; Gomez-Moron, M.A.; Ortiz, P. Nanoparticles Applied to Stone Buildings. *Int. J. Archit. Herit.* **2019**, 1–16. [[CrossRef](#)]
161. Chen, J.; Poon, C.S. Photocatalytic construction and building materials: From fundamentals to applications. *Build. Environ.* **2009**, *44*, 1899–1906. [[CrossRef](#)]
162. Dyshlyuk, L.; Babich, O.; Ivanova, S.; Vasilchenko, N.; Atuchin, V.; Korolkov, I.; Russakov, D.; Prosekov, A. Antimicrobial potential of ZnO, TiO₂ and SiO₂ nanoparticles in protecting building materials from biodegradation. *Int. Biodeterior. Biodegrad.* **2020**, *146*, 8. [[CrossRef](#)]
163. Chen, L.; Pan, H.; Zhuang, C.F.; Peng, M.Y.; Zhang, L. Joint wound healing using polymeric dressing of chitosan/strontium-doped titanium dioxide with high antibacterial activity. *Mater. Lett.* **2020**, *268*, 3. [[CrossRef](#)]
164. Chan, B.P.; Leong, K.W. Scaffolding in tissue engineering: General approaches and tissue-specific considerations. *Eur. Spine J.* **2008**, *17*, S467–S479. [[CrossRef](#)] [[PubMed](#)]

165. Malmir, S.; Karbalaee, A.; Pourmadadi, M.; Hamed, J.; Yazdian, F.; Navaee, M. Antibacterial properties of a bacterial cellulose CQD-TiO₂ nanocomposite. *Carbohydr. Polym.* **2020**, *234*, 10. [[CrossRef](#)] [[PubMed](#)]
166. Fan, X.L.; Chen, K.K.; He, X.C.; Li, N.; Huang, J.B.; Tang, K.Y.; Li, Y.J.; Wang, F. Nano-TiO₂/collagen-chitosan porous scaffold for wound repairing. *Int. J. Biol. Macromol.* **2016**, *91*, 15–22. [[CrossRef](#)]
167. Marulasiddeshwara, R.; Jyothi, M.S.; Soontarapa, K.; Keri, R.S.; Velmurugan, R. Nonwoven fabric supported, chitosan membrane anchored with curcumin/TiO₂ complex: Scaffolds for MRSA infected wound skin reconstruction. *Int. J. Biol. Macromol.* **2020**, *144*, 85–93. [[CrossRef](#)]
168. Ansarizadeh, M.; Haddadi, S.A.; Amini, M.; Hasany, M.; SaadatAbadi, A.R. Sustained release of CIP from TiO₂-PVDF/starch nanocomposite mats with potential application in wound dressing. *J. Appl. Polym. Sci.* **2020**, *137*, 11. [[CrossRef](#)]
169. Ashraf, R.; Sofi, H.S.; Akram, T.; Rather, H.A.; Abdal-Hay, A.; Shabir, N.; Vasita, R.; Alrokayan, S.H.; Khan, H.A.; Sheikh, F.A. Fabrication of multifunctional cellulose/TiO₂/Ag composite nanofibers scaffold with antibacterial and bioactivity properties for future tissue engineering applications. *J. Biomed. Mater. Res. A* **2020**, *108*, 947–962. [[CrossRef](#)] [[PubMed](#)]
170. Monmaturapoj, N.; Thepsuwan, W.; Mai-Ngam, K.; Ngermpimai, S.; Klinsukhon, W.; Prahsarn, C. Preparation and properties of hydroxyapatite/titania composite for microbial filtration application. *Adv. Appl. Ceram.* **2014**, *113*, 267–274. [[CrossRef](#)]
171. Li, Y.; Leung, P.; Yao, L.; Song, Q.W.; Newton, E. Antimicrobial effect of surgical masks coated with nanoparticles. *J. Hosp. Infect.* **2006**, *62*, 58–63. [[CrossRef](#)] [[PubMed](#)]
172. Jamróz, E.; Kulawik, P.; Kopel, P. The Effect of Nanofillers on the Functional Properties of Biopolymer-Based Films: A Review. *Polymers* **2019**, *11*, 675. [[CrossRef](#)] [[PubMed](#)]
173. Nazir, S.; Azad, Z.R.A.A. Food Nanotechnology: An Emerging Technology in Food Processing and Preservation. In *Health and Safety Aspects of Food Processing Technologies*; Springer: Cham, Switzerland, 2019; pp. 567–576.
174. Bajpai, V.K.; Kamle, M.; Shukla, S.; Mahato, D.K.; Chandra, P.; Hwang, S.K.; Kumar, P.; Huh, Y.S.; Han, Y.-K. Prospects of using nanotechnology for food preservation, safety, and security. *J. Food Drug Anal.* **2018**, *26*, 1201–1214. [[CrossRef](#)] [[PubMed](#)]
175. Hoseinnejad, M.; Jafari, S.M.; Katouzian, I. Inorganic and metal nanoparticles and their antimicrobial activity in food packaging applications. *Crit. Rev. Microbiol.* **2018**, *44*, 161–181. [[CrossRef](#)]
176. Sharma, R.; Jafari, S.M.; Sharma, S. Antimicrobial bio-nanocomposites and their potential applications in food packaging. *Food Control* **2020**, *112*, 11. [[CrossRef](#)]
177. Anaya-Esparza, L.M.; Ruvalcaba-Gomez, J.M.; Maytorena-Verdugo, C.I.; Gonzalez-Silva, N.; Romero-Toledo, R.; Aguilera-Aguirre, S.; Perez-Larios, A.; Montalvo-Gonzalez, E. Chitosan-TiO₂: A Versatile Hybrid Composite. *Materials* **2020**, *13*, 811. [[CrossRef](#)]
178. Goudarzi, V.; Shahabi-Ghahfarrokhi, I.; Babaei-Ghazvini, A. Preparation of ecofriendly UV-protective food packaging material by starch/TiO₂ bio-nanocomposite: Characterization. *Int. J. Biol. Macromol.* **2017**, *95*, 306–313. [[CrossRef](#)]
179. Bohmer-Maas, B.W.; Fonseca, L.M.; Otero, D.M.; Zavareze, E.D.; Zambiasi, R.C. Photocatalytic zein-TiO₂ nanofibers as ethylene absorbers for storage of cherry tomatoes. *Food Packag. Shelf Life* **2020**, *24*, 7. [[CrossRef](#)]
180. Youssef, A.M.; El-Sayed, S.M. Bionanocomposites materials for food packaging applications: Concepts and future outlook. *Carbohydr. Polym.* **2018**, *193*, 19–27. [[CrossRef](#)]
181. Zhang, X.D.; Xiao, G.; Wang, Y.Q.; Zhao, Y.; Su, H.J.; Tan, T.W. Preparation of chitosan-TiO₂ composite film with efficient antimicrobial activities under visible light for food packaging applications. *Carbohydr. Polym.* **2017**, *169*, 101–107. [[CrossRef](#)] [[PubMed](#)]
182. Lin, D.R.; Yang, Y.M.; Wang, J.; Yan, W.J.; Wu, Z.J.; Chen, H.; Zhang, Q.; Wu, D.T.; Qin, W.; Tu, Z.C. Preparation and characterization of TiO₂-Ag loaded fish gelatin-chitosan antibacterial composite film for food packaging. *Int. J. Biol. Macromol.* **2020**, *154*, 123–133. [[CrossRef](#)] [[PubMed](#)]
183. Xie, J.; Hung, Y.C. UV-A activated TiO₂ embedded biodegradable polymer film for antimicrobial food packaging application. *LWT-Food Sci. Technol.* **2018**, *96*, 307–314. [[CrossRef](#)]
184. Hong, L.; Luo, S.H.; Yu, C.H.; Xie, Y.; Xia, M.Y.; Chen, G.Y.; Peng, Q. Functional Nanomaterials and Their Potential Applications in Antibacterial Therapy. *Pharm. Nanotechnol.* **2019**, *7*, 129–146. [[CrossRef](#)] [[PubMed](#)]

185. Teymourpour, S.; Mohammadi Nafchi, A.; Nahidi, F. Functional, thermal, and antimicrobial properties of soluble soybean polysaccharide biocomposites reinforced by nano TiO₂. *Carbohydr. Polym.* **2015**, *134*, 726–731.

Publisher's Note: MDPI stays neutral with regard to jurisdictional claims in published maps and institutional affiliations.



© 2020 by the authors. Licensee MDPI, Basel, Switzerland. This article is an open access article distributed under the terms and conditions of the Creative Commons Attribution (CC BY) license (<http://creativecommons.org/licenses/by/4.0/>).